Advanced Drug Delivery Reviews 104 (2016) 44–60

Contents lists available at ScienceDirect

Advanced Drug Delivery Reviews

journal homepage: www.elsevier.com/locate/addr

Imaging-guided delivery of RNAi for anticancer treatment☆

Junqing Wang [a,b,1], Peng Mi [a,c,1], Gan Lin [a,1], Yì Xiáng J. Wáng [b,*], Gang Liu [a,d,e,*], Xiaoyuan Chen [f,*]

[a] State Key Laboratory of Molecular Vaccinology and Molecular Diagnostics and Center for Molecular Imaging and Translational Medicine, School of Public Health, Xiamen University, Xiamen 361102, China
[b] Department of Imaging and Interventional Radiology, Faculty of Medicine, Prince of Wales Hospital, The Chinese University of Hong Kong, Shatin, Hong Kong, China
[c] Chemical Resources Laboratory, Polymer Chemistry Division, Tokyo Institute of Technology, R1-11, 4259 Nagatsuta, Midori-ku, Yokohama 226-8503, Japan
[d] State Key Laboratory of Cellular Stress Biology, Innovation Center for Cell Biology, School of Life Sciences, Xiamen University, Xiamen, 361102, China
[e] The MOE Key Laboratory of Spectrochemical Analysis and Instrumentation, College of Chemistry and Chemical Engineering, Xiamen University, Xiamen, 361005, China
[f] Laboratory of Molecular Imaging and Nanomedicine, National Institute of Biomedical Imaging and Bioengineering, National Institutes of Health, Bethesda, MD 20892, USA

ARTICLE INFO

Article history:
Received 2 April 2015
Received in revised form 27 November 2015
Accepted 13 January 2016
Available online 22 January 2016

Keywords:
Molecular imaging
Cancer
Nanocarrier
siRNA
RNA interference
Gene delivery
Theranostics

ABSTRACT

The RNA interference (RNAi) technique is a new modality for cancer therapy, and several candidates are being tested clinically. In the development of RNAi-based therapeutics, imaging methods can provide a visible and quantitative way to investigate the therapeutic effect at anatomical, cellular, and molecular level; to noninvasively trace the distribution; to and study the biological processes in preclinical and clinical stages. Their abilities are important not only for therapeutic optimization and evaluation but also for shortening of the time of drug development to market. Typically, imaging-functionalized RNAi therapeutics delivery that combines nanovehicles and imaging techniques to study and improve their biodistribution and accumulation in tumor site has been progressively integrated into anticancer drug discovery and development processes. This review presents an overview of the current status of translating the RNAi cancer therapeutics in the clinic, a brief description of the biological barriers in drug delivery, and the roles of imaging in aspects of administration route, systemic circulation, and cellular barriers for the clinical translation of RNAi cancer therapeutics, and with partial content for discussing the safety concerns. Finally, we focus on imaging-guided delivery of RNAi therapeutics in preclinical development, including the basic principles of different imaging modalities, and their advantages and limitations for biological imaging. With growing number of RNAi therapeutics entering the clinic, various imaging methods will play an important role in facilitating the translation of RNAi cancer therapeutics from bench to bedside.

Published by Elsevier B.V.

Contents

☆ This review is part of the *Advanced Drug Delivery Reviews* theme issue on "RNAi clinical translation".

* Corresponding authors.
E-mail addresses: yixiang_wang@cuhk.edu.hk (Y.X.J. Wáng), gangliu.cmitm@xmu.edu.cn (G. Liu), shawn.chen@nih.gov (X. Chen).

[1] These authors contributed equally.

http://dx.doi.org/10.1016/j.addr.2016.01.008
0169-409X/Published by Elsevier B.V.

1. Introduction

Since it was discovered that double-stranded RNA (dsRNA) can induce RNA interference (RNAi) in *Caenorhabditis elegans* [1], the capability of RNAi that can suppress the expression of target genes with high specificity, and efficacy has been confirmed with small RNA sequences (siRNA/miRNA) [2]. Since then, much effort has been directed to develop RNAi therapeutics into clinic as a potential disruptive tool for new conservative and personalized treatment of a broad range of diseases [3], including viral infection [4], eye disorder [5], inflammatory disease [6], cardiovascular disease [7], genetic disorder [8], and cancer [9–11].

Currently, both naked siRNAs and nanoparticle-mediated delivery of RNA fragments have been investigated for cancer therapy. The administration route for naked siRNA is critically reliant on its accessibility to the target sites inside the body. Most of the naked siRNA fragments have been administered topically, which has the advantages of high bioavailability in target organs and low adverse reactions compared to systemic administration. Because the systemic administration of siRNA fragments requires them to reach the right organs or tissues after dispersing in the body and passing through the biological barriers, which is virtually impossible for naked small RNAs. The systemic delivery of siRNAs or other small therapeutic RNAs to target sites is impeded by many factors including nuclease degradation and rapid systemic elimination of "naked" small RNAs in biological systems [12]; intrinsic negative charge nature on the surface of small RNAs make them very difficult to transfer into cells that also with negatively charged surface of bilayer phospholipid membrane [13]. Therefore, a variety of delivery systems have been engineered to address above issues and deliver small RNAs specifically to target sites, including tumors and inflammatory foci, for instance, lipid nanoparticles made with cationic lipids; lipidol and other lipid materials [14–17]; polymeric nanoparticles made with polyethylenimine (PEI); dendrimers; membrane-disruptive and cyclodextrin-containing polymers [18–20]; membrane-disruptive peptides [21,22]; aptamer-siRNA chimeras [23]; single-chain fragmented antibodies [24]; supramolecular assemblies [25–27]; inorganic nanoparticles, including multishell nanoparticles, mesoporous nanoparticles, and carbon-based nanomaterials [28]; and so on [29–33]. However, the entrapment of nano-sized carriers in the reticuloendothelial system (RES), the vascular endothelial resistance in tissues, the barriers of extracellular matrix, and the intracellular release from endosomal uptake [34,35] are the major challenges for the systemic delivery of RNAi therapeutics. In addition, the siRNA-based therapeutics encounter safety concerns owing to unexpected adverse effects, including off-target effects, innate immune responses, proinflammatory cytokine induction, and spleen toxicity, which were found in the early studies of those candidates [8,36–38].

There are three major aspects of scientific challenges in developing RNAi therapeutics for cancer therapy (Fig. 1): (1) target gene selection for RNAi and gene vector development for either systemic or local administration; (2) product screening and preclinical evaluation including the relative efficacy, biodistribution, pharmacokinetics, and toxicity; and (3) clinical study of the efficacy, safety, pharmacokinetics, and optimal dose. It has been proven that noninvasive imaging methods and biomarker detection could speed up the development of RNAi therapeutics [39–41]. Developing powerful imaging techniques and methods is important for providing valuable information by visualizing, characterizing, and quantifying the biological processes of RNAi therapeutics and monitoring their therapeutic effects and factors that are crucial for the optimization of RNAi cancer therapeutics.

Generally, *in vivo* imaging of RNAi refers to the utilization of a variety of imaging modalities, including bioluminescence imaging (BLI) [42], photoluminescence imaging [43,44], magnetic resonance imaging (MRI) [45], positron emission tomography (PET) [46], single-photon emission computed tomography (SPECT) [47], and ultrasound [48], to quantitatively and/or qualitatively visualize the *in vivo* behavior of the RNAi therapeutics. Many imaging modalities have been applied for RNAi researches. The therapeutic genes have been directly or indirectly marked with a variety of imaging contrast agents to make them detectable in biological systems with clinically relevant imaging equipment. These probe-labeled systems with target delivery function hold high promise for studying the pharmacological properties of RNAi therapeutics in clinical translation. This review highlights the current status of RNAi-based cancer therapeutics in clinical trials with discussion of selected cases. Before addressing the current progresses of applying

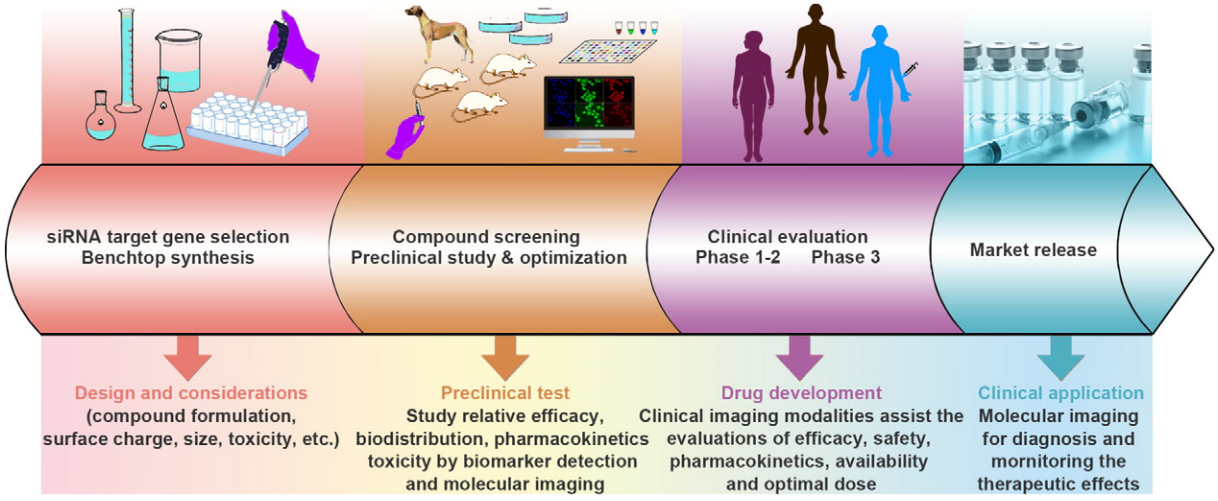

Fig. 1. The workflow of developing RNAi therapeutics and translating them for clinical applications. There are mainly four steps for this, including targeting gene selection, compound screening, clinical evaluation, and market release. Imaging methods could assist the development of RNAi therapeutics at every step in the RNAi therapeutics development processes, including marking for gene selection, tracing the small RNA sequences for pharmacokinetics study, evaluating the gene-silencing efficacy, and diagnosing tumors and monitoring the therapeutic effects.

various imaging techniques in RNAi therapeutics development, we will discuss the biological barriers and challenges for developing RNAi therapeutics and emphasize the design considerations of non-viral gene delivery vehicles for targeting tumors. Finally, the perspective of applying various imaging techniques for developing RNAi cancer therapeutics is described in more detail.

2. RNAi cancer therapeutics in clinical trials

The significant advantages of RNAi strategy are its high specificity together with infinite choice of genes that can be applied for cancer therapy. The RNAi therapeutics could interfere with angiogenesis, metastasis, chemoresistance of tumors, and the proliferation of cancer cells [49,50]. The intrinsic features of RNAi therapeutics make RNAi a novel strategy for cancer treatment. Therefore, a myriad of RNAi therapeutics is under investigation for this purpose. Recently, around 10 types of RNAi-based cancer therapeutics have entered the early stage of clinical trial (Table 1), demonstrating potential capability of RNAi with specific gene-silencing efficacy for cancer treatment. Although the ongoing clinical trials provide encouraging results for future commercial success, many obstacles still remain ahead for applying RNAi therapeutics in humans. Here, we highlight the current status of two selected cases in clinical evaluation.

The siRNA-loaded lipid nanoparticles (Atu027) have been applied clinically to suppress the expression of protein kinase N3 (PKN3) [63]. PKN3 is an effector of PI3K pathway related to the modulation of cell growth, differentiation, survival, motility, and adhesion as well as immune cell and glucose transport function. Chronic activation of PI3K pathway could prevent various human cancers and inhibit the growth of malignant cells [64]. Although numerous signaling molecules can be considered as therapeutic candidates to mediate the PI3K pathway, their upstream inhibition could trigger signal cascades with undesirable signal regulation of normal cells associated with various side effects. For this reason, PKN3 is considered to be a proper effector to adjust the growth of metastatic cancer cells with activated PI3K [65]. The results from animal studies indicate that Atu027 could effectively knock down the expression of PKN3 gene in the vascular endothelium to inhibit tumor growth and metastasis [63]. In clinical study of Atu027, no interferon response or activation of cytokines was observed, which may be due to liposomal encapsulation of siRNA with enhanced safety while avoiding triggering side reactions during circulation [66]. Thus, Atu027 was well tolerated, and no dose-dependent toxicity was observed. Recent study of using Atu027 to treat advanced solid tumors has found that up to 41% of patients exhibited no further progression of tumors after eight weeks of treatment [67]. Since Atu027 targets tumor stroma instead of tumor cells, it is expected that this treatment will be effective for all type of vascularized metastatic cancers.

Another clinical trial product that targets kinesin spindle protein (KSP) and vascular endothelial growth factor (VEGF) for treating solid tumors is ALN-VSP02. KSP is a type of motor protein that plays a central role in the proper separation of emerging spindle poles during mitosis, and it is upregulated in many types of cancer cells. Therefore, KSP is another attractive target for cancer therapy by RNAi therapeutics, as silencing its expression will lead to cell cycle arrest at mitosis through the formation of an abnormal mitotic spindle and finally inducing apoptosis [68]. VEGF, which is involved in angiogenesis and lymphangiogenesis, is overexpressed in numerous cancer types [69,70]. Blocking the expression of VEGF is expected to inhibit angiogenesis and suppress tumor growth [71]. The dually targeted RNAi drug (ALN-VSP02) is in clinical trial aimed for treating solid tumors (Fig. 2a). In the first-in-human study, the clinical activity, safety, and pharmacokinetics of ALN-VSP02 were evaluated, demonstrating good systemic tolerance and acceptable toxicity with biweekly intravenous administration. The results also demonstrated that the expression levels of both target genes were decreased in multiple patients, including one patient with complete regression of liver metastases from endometrial cancer (Fig. 2b, c) [11]. Although ALN-VSP02 has achieved some success in clinical trials, some interesting results should be noticed. The infusion-related reactions (IRR) of ALN-VSP02 seem to be complement-mediated, not cytokine-induced. Additionally, it was found that ALN-VSP02 could cause spleen toxicity with prolonged dosing. The patient with endometrial cancer had a more than 50% decrease in blood flow (K_{trans}) and a 90% reduction in spleen size [11]. Based on the above observations, some improvements are suggested for future development of Stable nucleic acid lipid particle (SNALP)-based cancer siRNA therapeutics to improve the safety. It includes using more efficacious and less immunogenic lipid components and reducing the size of SNALP-based drug delivery systems to be small enough to improve the circulation time and benefit the accumulation in solid tumors through the enhanced permeability and retention (EPR) effect. Finally, the biodegradability of SNALP should be optimized to reduce the spleen toxicity, which was induced by lipid accumulation along the endosomal-lysosomal pathway.

To date, owing to the low stability, poor systemic distribution, possible side reactions, and low bioavailability of naked siRNA, most siRNA-

Table 1
Current clinical status of RNAi therapeutics for cancer treatment.

Indications	Name	Delivery Route	Target	Delivery system	Development phase	References
Advanced solid tumors	siRNA-EphA2-DOPC	Intravenous injection	EphA2	Lipid-based nanoparticles	Preclinical	[51]
Metastatic tumors or cannot be removed by surgery	APN401	Intravenous injection	E3 ubiquitin ligase Cbl-b	*Ex vivo* transfection	Preclinical	[52]
Metastatic melanoma, absence of CNS metastases	iPsiRNA	Intradermal injection	LMP2, LMP7, MECL1	*Ex vivo* transfection	Phase I, completed	[53]
Advanced solid tumors	Atu027	Intravenous infusion	PKN3	Lipid-based nanoparticles	Phase I, completed	[54]
Pancreatic ductal adenocarcinoma; Pancreatic cancer	siG12D LODER	Intratumoral implantation	KRASG12D	LODER polymer	Phase I, completed	[55]
Primary or secondary liver cancer	TKM-080,301	Hepatic intra-arterial injection	PLK1	Lipid-based nanoparticles	Phase I, completed	[56]
METAVIR F3-4	ND-L02-s0201	Intravenous injection	HSP47	Lipid-based nanoparticles	Phase I, recruiting	[57]
Solid tumors; multiple myeloma; non-Hodgkin's lymphoma	DCR-MYC	Intravenous infusion	MYC	Lipid-based nanoparticles	Phase I, recruiting	[58]
Cancer; solid tumor	CALAA-01	Intravenous injection	RRM2	cyclodextrin-containing polymer	Phase I, terminated	[59]
Neuroendocrine tumors; adrenocortical carcinoma	TKM 080301	Intravenous infusion	PLK1	Lipid-based nanoparticles	Phase I/II, recruiting	[60]
Solid tumors	ALN-VSP02	Intravenous injection	KSP, VEGF	Lipid-based nanoparticles	Phase I, completed	[61,62]

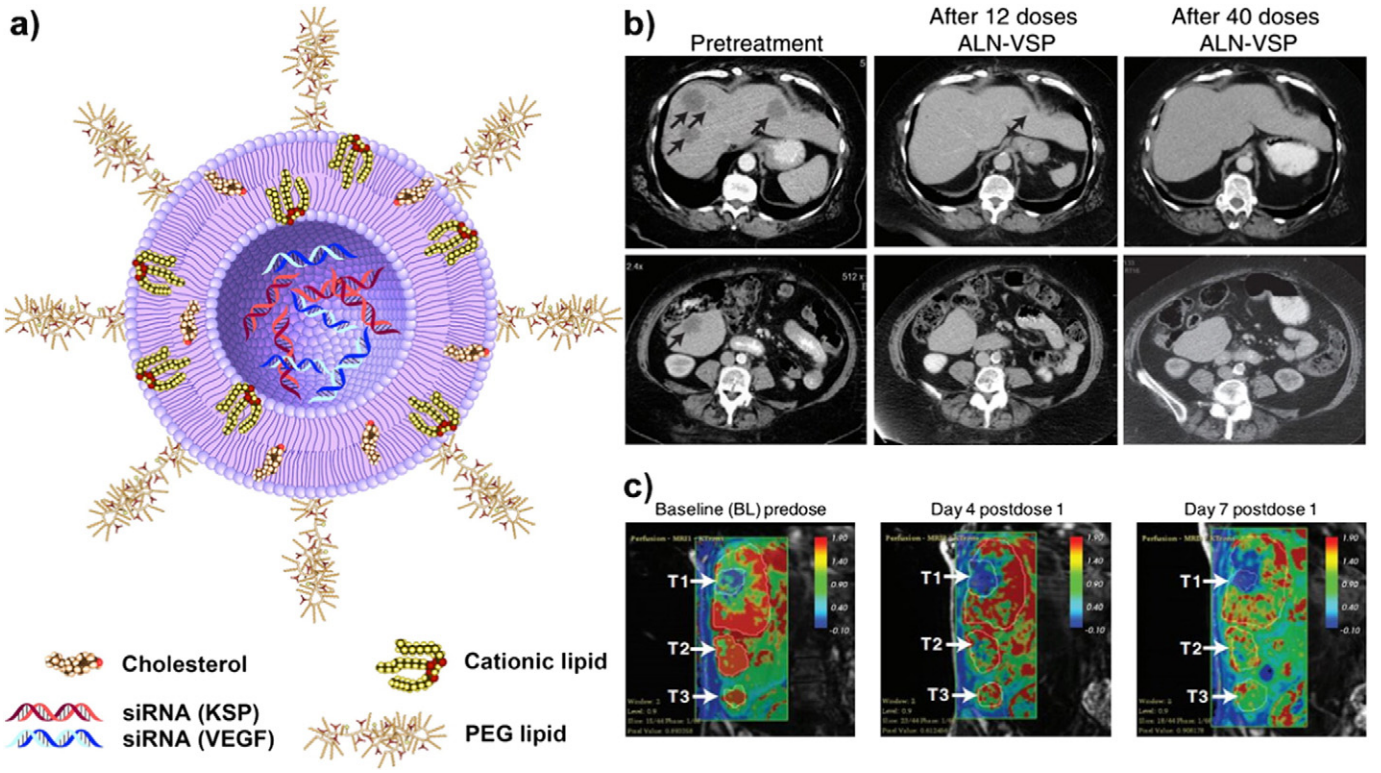

Fig. 2. (a) Schematic structure of ALN-VSP formulation: The siRNA lipid nanoparticle is composed of cationic or ionizable lipid with cholesterol and encapsulated with two different siRNAs to target KSP and VEGF genes. The nanoparticles are stabilized by surface binding of PEGylated lipids. (b) CT images demonstrated a complete response of ALN-VSP in an endometrial cancer patient with multiple liver metastatic tumors (black arrows). (c) Dynamic contrast-enhanced MRI (DCE-MRI) images from another patient with three metastatic pancreatic neuroendocrine tumors in the right lobe of the liver (white arrows). A significant change of tumor blood flow was observed during the treatment at 0.7 mg/kg (indicated in red). Figures adapted with permission from [11].

based therapeutics in clinical trials are formulated by encapsulation within lipid-based particles. These early trials hold great potential for cancer therapy, especially allowing RNAi to be precisely tailored in each case. However, many challenges still need to be solved for personalized cancer therapy by RNAi to become a reality. First, RNAi delivery systems with high efficiency and low toxicity are needed for early (Phase I) clinical trial. Then an adequate knockdown of target genes needs to be achieved in later trials of Phase I to Phase II. Besides, possible off-target effects in normal tissues should be avoided for safety consideration (Phase II). The positive or negative correlation of target knockdown with tumor regression should be analyzed during Phase II to verify the feasibility for Phase III study. Finally, for future clinical applications, the distribution, metabolism, and degradation of siRNA-loaded nanocarriers need to be extensively studied.

3. Biological barriers for RNAi cancer therapeutics

Although several siRNA-based therapeutics have been evaluated in early phase clinical studies, there are various biological barriers that need to be conquered for successful clinical translation, such as efficient delivery of RNAi therapeutics to tumors after reaching the circulation, overcoming the vascular barrier, cellular uptake, and endosomal escape (Fig. 3). Because many target sites are not accessible or not convenient for local administration, thus the systemic administration of RNAi therapeutics is essential. To fully exploit the therapeutic potential of RNAi therapeutics, developing effective and biocompatible gene delivery systems that could specifically target cancer cells in the body is a key factor. Generally, gene vehicles with the diameter ranging from 10 to 100 nm are suitable for systemic administration. These gene vectors are needed to be stable enough and well dispersed in blood. Besides, gene vectors decorated with targeting moieties could facilitate specific cellular uptake by cancer cells, a strategy that is important to evade the innate immune stimulation in the body [72]. In such cases, noninvasive imaging tools can be utilized to study the pharmacokinetic properties of RNAi therapeutics and monitor their effects in a visible way. In order to accelerate the screening process, imaging techniques with adequate spatial resolution and sensitivity for small animals should be used for determining the temporal and spatial biodistribution of the developed compounds. This may help reduce irrational costs and allow the selection of the most promising candidates during the early stage of drug development [73].

3.1. Administration barrier

Administration through oral route is obviously the most convenient approach for patients. However, it is currently challenging for treating cancers through the oral administration of RNAi therapeutics due to difficulties in accessing tumor sites, including poor intestinal stability and insufficient permeability across intestinal epithelium into circulation [34]. Subcutaneous administration is another route for the systemic delivery of RNAi therapeutics. The drugs can reach the circulation directly from the interstitial space of subcutaneous connective tissue to the capillaries by traversing through the vascular barrier or through lymphatic drainage. Compared to intravenous administration, the sustained entry of drugs into circulation through subcutaneous route can achieve almost complete absorption without first-pass effect in the liver. A clinical example of RNAi therapeutics using subcutaneous administration to treat transthyretin-mediated amyloidosis is ALN-TTRsc, which could achieve approximately 90% knockdown of the transthyretin gene expression in liver in a phase I study [74]. For the subcutaneous administration of RNAi therapeutics, the lipophilicity and size of gene vectors have to be taken into account to avoid endocytosis by phagocytic cells in subcutis and lymph node drainage, which subsequently influence the potency of RNAi therapeutics. For further details on designing desirable properties of siRNA delivery system, please refer to the following

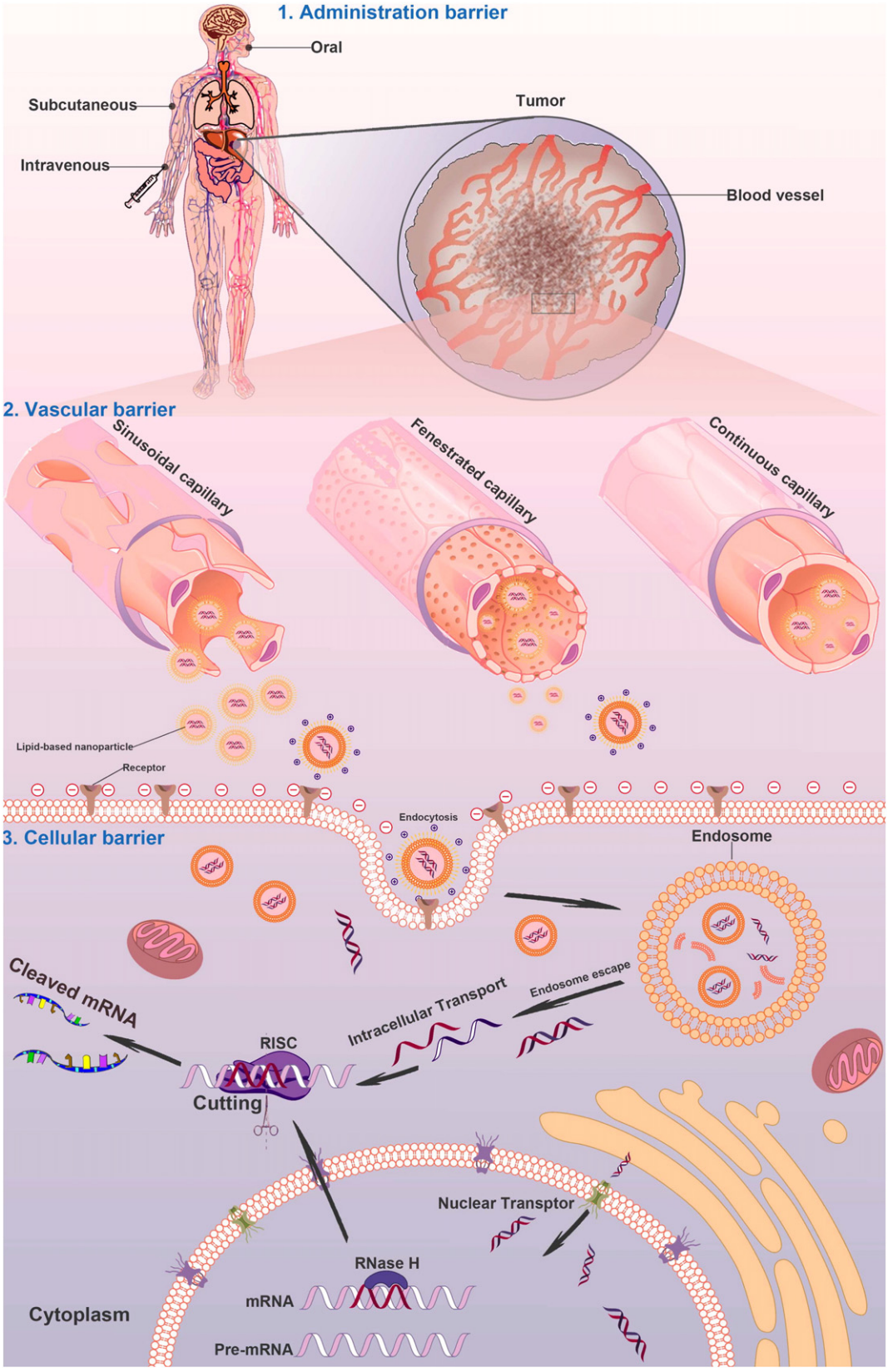

Fig. 3. Schematic illustration of nanocarrier-mediated delivery of RNAi therapeutics: the biological barriers for gene silencing in cancer treatment include reaching the circulation, crossing the vascular barrier, cellular uptake, and endosomal escape. Following systemic administration in patients, the RNAi therapeutics could be transported to the blood vessels in tumor tissues. The gene vectors could escape from the sinusoidal and fenestrated capillaries and retain in the tumor regions. The gene vectors could be taken by cancer cells through endocytosis or ligand-mediated intracellular transport and then transferred into the cytoplasm to silence target genes for cancer therapy.

reviews [17,19,75–79]. The most direct way for RNAi therapeutics to reach blood circulation is intravenous or infusion injection. Currently, several RNAi products for systemic administration have entered clinical evaluation for cancer treatment (Table 1). In order to identify and validate gene vector candidates for specific administration route of siRNA delivery during preclinical stage, *in vitro* and *in vivo* optical imaging can be assisted as a fast and inexpensive method for compound screening by visualizing and evaluating the biocompatibility, stability, absorption, and distribution in a live subjects in a real-time manner, as well as biological interactions at subcellular level.

3.2. Vascular barrier

Passing through the endothelium of vasculature is a key step for RNAi therapeutics. Depending on the vascular permeability of target organs or tissues, a certain half-life of RNAi therapeutics in plasma is required. A successful gene silencing in the liver primarily benefits from the discontinuous sinusoidal capillaries, as the large openings in the endothelium can greatly access the leaked RNAi nanocarriers from the vasculature. Such pores in sinusoidal capillaries are wide openings for both passive and active passages of RNAi nanocarriers up to 100 nm in size from bloodstream to hepatocytes in liver. Tumor capillaries are discontinuous, with considerable variation of cell composition, the basement membrane, and pericyte coverage. Kobayashi et al. suggested that four important factors should be considered when passive targeting is involved [80]: (1) internal and external blood flow of tumor, (2) tumor vascular permeability, (3) structural barriers enforced by extracellular matrix and tumor cells, and (4) intratumoral interstitial pressure. These factors can certainly influence the accumulation of certain sized nanoparticles or molecules in tumor tissue by EPR effect [81]. In order to take advantage of the EPR effect in tumor tissues, or receptor-mediated transcytotic pathway through vascular endothelium [34], longer half-life for RNAi therapeutics is necessary. In contrast to sinusoidal or tumor capillaries, the fenestrated capillaries have much smaller pores (60–80 nm in diameter) in endothelium covered with continuous basal lamina, which can prevent the diffusion of large-scale nanoparticles. They are mainly located in the endocrine glands, intestines, pancreas, and glomeruli of kidneys. The tightness, shape of the pores, continuous basal lamina, and extracellular matrix should be considered for designing non-hepatic tissues-targeted RNAi-based formulations and delivery strategies.

The stability of RNAi therapeutics in blood circulation is of primary importance for arriving tumor tissues. A major challenge is to evade the phagocytic uptake by mononuclear phagocyte system (MPS) in the bloodstream [82]. The formulation size, surface electrostatic nature, and stability can certainly affect the uptake by MPS. It is more likely to interact with MPS and other components in the bloodstream if they possess large size and excessive net charge [83]. Thus, the formulations are generally of minimum net charge through modification with hydrophilic and neutral molecules to increase the stability. Introducing poly(ethylene glycol) (PEG) shell to the surface of RNAi vectors is a general approach for stabilization. However, the high stability achieved by PEGylation can reduce uptake by target cells [84]. This can be solved by attaching targeting moieties to RNAi therapeutics [85]. The vascular endothelium is negatively charged because the heparin sulfate proteoglycans are on the cell surface and in the extracellular matrix. Additionally, tumor vascularity is controlled by oxygen supply and some metabolites [86]. It has been observed that increasing the tumor vascularity could result in more efficient delivery of RNAi agents to solid tumors [87]. It was reported that nanoparticles with smaller size and increased lipophilicity could lead to higher level of accumulation in tumor tissues [88]. To evaluate the delivery efficiency and *in vivo* behavior of the potential RNAi therapeutics, quantitative functional, and molecular imaging can be integrated to provide valuable information concerning pharmacokinetics and biodistribution properties in animal models, such as quantitative visualization of compound absorption and distribution in tissues and organs, as well as elimination time after the administration, and the amount of compounds that reaching target tissues. Usually, the quantitative imaging assessment can be performed in a real-time, whole-body, and noninvasive way by selecting appropriate imaging techniques. In this method, the compound is often labeled with specific imaging probes corresponding to the imaging modality for further applications. A great benefit of this approach is that the animals can be imaged repeatedly for longitudinal studies, which minimizes the number of animals needed for a given experiment [89].

3.3. Cellular barrier

Cellular uptake is critical for successful delivery of RNAi therapeutics into the cytoplasm for gene silencing. Basically, cell membrane is comprised of hydrophobic phospholipid bilayer embedded with various functional proteins. The innate negatively charged cell surface provides an external biological barrier to naked siRNA molecules. The small cationic peptides, cationic lipids, and polymers have often been applied to facilitate the cellular uptake of siRNA molecules *via* endocytosis [90]. However, for targeted delivery of RNAi therapeutics into cancer cells, the receptor-mediated endocytosis is mostly preferred, and various ligands have been used for targeted delivery of RNAi therapeutics, including folate [91], transferrin [92], and aptamers [93]. Those ligands could specifically interact with receptors overexpressed on the surface of cancer cells to promote cellular uptake. Pros and cons of using various targeting ligands for siRNA therapeutics have been reviewed elsewhere [94]. Once entering into target cells, the success in approaching RNA-induced silencing complex (RISC) in cytoplasm is largely dependent on endosomal escape. It has been suggested that endosomal escape should occur before late endosomes fuse with lysosomes, which contains certain digestive enzymes [95]. For cationic polymers, which could enhance endosomolysis *via* absorbing protons and preventing the acidification of the endosomes, the elevated influx of the protons to endosomes increases osmotic pressure that causes lysosome swelling and rupture, eventually releasing the gene vectors to cytoplasm [96,97]. Similarly, ionizable lipids with neutral charge in bloodstream can become positively charged in endosomes, subsequently leading to disruption of the endosome membrane [17]. Elucidating the mechanism of endosomal escape pathways can help develop new strategies for gene delivery without relying on acidification. For investigations of cellular uptake and intracellular trafficking, molecular/cellular imaging is an essential tool to demonstrate the ligand-receptor interaction, subcellular translocation, and mechanism of potential RNAi therapeutics. Fluorescent probes and radioactive isotope-labeled drug candidates are commonly used for whole-body and subcellular tracking to provide quantitative and qualitative information of biological processes occurring at cellular and molecular levels.

3.4. Immune response and safety

The key issue in the application of RNAi therapeutic is the safety without any undesirable side effects. Unwanted silencing of target genes in normal organs or tissues is called “off-target silencing” [38,98]. The siRNAs longer than 30 bp can induce the interferon pathway [36]. Such induction of interferon reaction is caused by the innate immune system because the human body recognizes long dsRNA as virus particles and triggers the innate immune system to overcome the infection. Several investigations showed that even low concentration of siRNAs can induce natural immunity by activating interferon expression [99]. It is suggested that the main mechanisms of immune response caused by some siRNAs are the stimulated production of pro-inflammatory cytokines through TLR-8 on monocytes and TLR-7 on dendritic cells in a sequence-dependent manner [36,100]. In order to overcome this problem, the therapeutic siRNAs should be less than

21–23 bp [36]. Chemical modifications including 2′-*O*-methylation are also performed to avoid immune activation of siRNAs. Hence, immunostimulatory effects of potential siRNA-based therapeutics must be evaluated in animals prior to the clinical trial until the exact mechanism of sequence-dependent siRNA-induced immune response is fully understood [101].

In addition to siRNA-induced immune activation, the formulation of siRNA-based nanoparticles also plays an important role in safety profile for systemic delivery. Presently, the collective results of siRNA SNALP-based nanoparticles (ALN-VSP), cationic liposome/lipoplexes (Atu027), and cyclodextrin-based polymers (CALAA-01) have shown RNAi efficacy and dose tolerability in early clinical development. Based on these valuable outcomes and lessons learned, several additional key investigations are suggested here. (1) The quality control assay for RNAi products must be performed to prevent structure alteration during the practical use. (2) A better understanding of proinflammatory cytokine response is needed for developing more potent siRNA-based nanoparticles with less acute immunostimulatory events. The side effects could be reflected in the change of pathological states or pathological indicators, such as inflammation, enzyme levels, and other biological factors. (3) Imaging techniques could be applied to study the safety of RNAi therapeutics. Once the safety evaluation of a potential RNAi therapeutic has been established in early trial, molecular imaging can assist in the establishment of biological activity at appropriate dosage range with acceptable toxicities associated with the detection, diagnosis, evaluation, treatment, and management of cancer.

4. Imaging modalities in the RNAi cancer therapeutics development process

Noninvasive imaging techniques are important tools to visualize and quantify the biological processes of RNAi therapeutics at cellular or tissue levels in a real-time way. Imaging-guided delivery of RNAi therapeutics can trace the pathway of RNAi therapeutics inside the body, provide pathological information of tumors, evaluate the tumor-targeted delivery, and provide further information about the pharmacokinetics of the RNAi therapeutics.

4.1. Optical imaging

Optical imaging, mainly including fluorescence imaging and bioluminescence imaging (BLI), which provides the most convenient way for preclinical study of RNAi knockdown due to their advantages including abundant choices of optical dyes, easy labeling, noninvasiveness, multi-channel imaging function, and whole-body real-time readout. Besides, the excellent sensitivity and inexpensive use of optical imaging (with maximum penetration depth of few centimeters [102,103]) make it a promising modality for real-time monitoring of siRNA delivery in small animals.

For fluorescence imaging, the animals are illuminated by a light at an appropriate wavelength to excite the fluorescent agents *in situ*, and then the emitted light from fluorescent agents is filtered and detected by a charge-coupled device (CCD) camera maintained at low temperature (Fig. 4a) [104]. Since both the excitation and emission lights used are low-energy photons, it is considerably safer than other imaging systems that involve ionizing radiation. However, the use of relatively low-energy light results in limited tissue penetration due to the light absorption by tissue components, which makes it virtually impossible for deep tissue imaging in large animals or human subjects. Moreover, there are other intrinsic limitations for consideration, for example, the light scattering phenomenon during the light propagation in tissues can result in a blurry fluorescence image [105]. For *in vivo* optical imaging, autofluorescence is an undesired background signals emitted by natural fluorophores in tissues, which can overlay with fluorescent signal from optical probes, and consequently reduce the signal-to-noise ratio [105]. Near-infrared fluorescent (NIRF) agents are generally applied for labeling siRNA therapeutics, as NIRF emits light in the range of 650–900 nm with deep tissue penetration by minimizing the tissue absorption, scattering, and autofluorescence [106]. For instance, VEGF siRNAs labeled with cyanines dye (Cy5.5) were conjugated to PEG through disulfides to form micelles through the interaction with PEI [107]. With Cy5.5, the VEGF siRNA-loaded micelles could be traced for delivering siRNA into prostate cancer cells (PC3), and the accumulation of Cy5.5-labeled siRNA, siRNA/PEI mixture and micelles could be detected in tumors and the main organs also could be monitored after

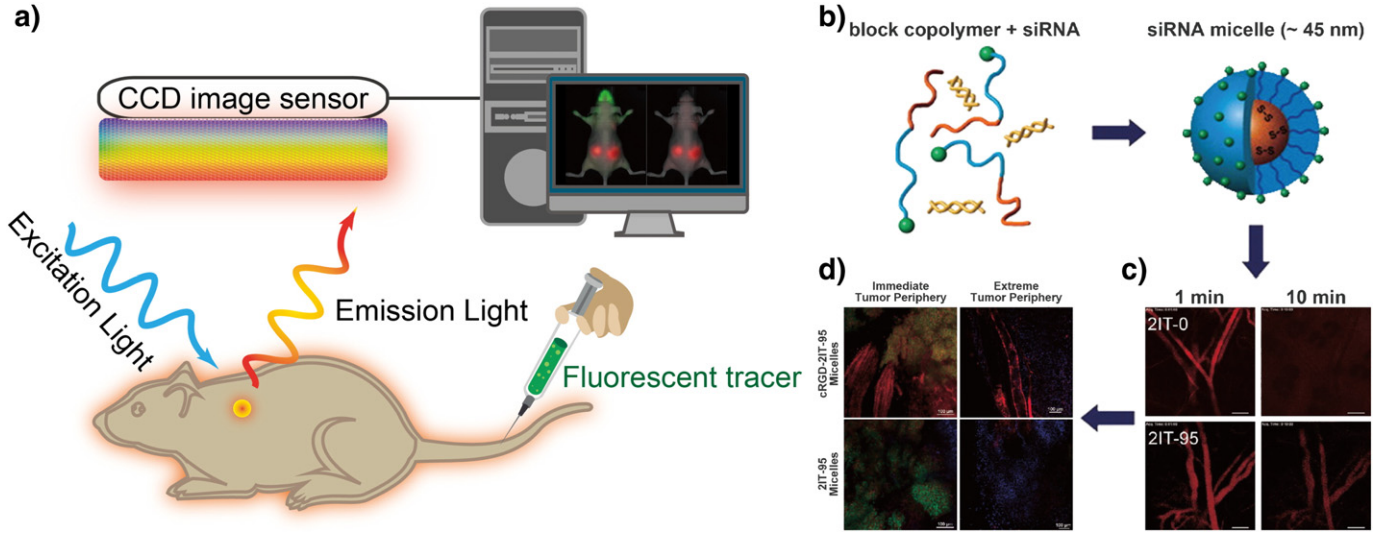

Fig. 4. Optical fluorescence imaging. (a) A schematic illustration of the basic principle of *in vivo* fluorescence imaging. First, a fluorescently labeled RNAi therapeutics is injected into mouse body, and the subject is illuminated by an excitation light at specific wavelength, resulting an excitation of fluorescent molecules and subsequent emission light of different wavelength. The emitted light is filtered and then detected by CCD image sensor. The fluorescence signals and animal photo are finally converted to a single detailed image. The figures on right show using fluorescence imaging to trace polymeric micelles incorporated with dye-labeled siRNA in the mice body. (b) Schematic illustration of polymeric micelle structure formed by self-assembly of block copolymers with fluorescent dye-labeled siRNA. (c) Ear-lobe dermis snap-shots of blood circulation of two types of micelles after intravenous injection for 1 and 10 min. (d) Micro distribution of micelles incorporated with Cy5-labeled siRNA at 24 h post-injection. (red: siRNA; green: tumor cell nuclei; purple: other cell nuclei). Figures adapted with permission from [110].

administration to PC-3 tumor-bearing mice. The fluorescent dyes could also be utilized to study the intracellular pathway of RNAi therapeutics. By image-based analysis of lipid nanoparticles (LNPs) incorporating A647-labeled siRNA, it was observed that the LNPs could enter cancer cells through clathrin-mediated endocytosis and macropinocytosis, while the efficiency of siRNA escape from endosome to cytosol was low (1–2%) and the endosome escape only occurred when the LNPs were located in the compartment sharing early and late endosomal characteristics [108]. In addition, fluorescence imaging could provide multi-channel imaging functions by labeling RNAi therapeutics with multiple dyes. For instance, the Cy3 and Cy5-labeled siRNAs were covalently linked to PEG to form nanocarrier-like loop, which could generate signals for dual imaging of the products inside cancer cells based on the fluorescence resonance energy transfer (FRET) of the fluorophore pair [109]. Furthermore, the RNAi therapeutics in blood circulation, leakage from blood to tumor tissues as well as distribution in tumor tissues can be monitored in a real-time manner with intravital confocal laser scanning microscopy (IVRTCLSM). For instance, the Cy5-siRNA-incorporated polymeric micelles and naked siRNA (Cy5-siRNA) could be traced in blood circulation to study their pharmacokinetics *in vivo*, to investigate their entry from blood to tumor tissues, as well as their distribution in tumor tissues by utilizing IVRTCLSM (Fig. 4b, c, d) [110–112].

Besides organic fluorescent dyes, other nanomaterials, such as quantum dots (QDs) [113], carbon dots (C-dots) [114], and up-converting nanoparticles (UCNPs) [115], are also used for optical imaging as well as for siRNA delivery due to their high signal intensity and photostability. Specifically, tumor-specific, multifunctional siRNA-loaded QDs were prepared to induce downregulation of the expression of epidermal growth factor receptor variant III (EGFRvIII), which plays an important role in interfering with the proliferation of various types of cancer cells, while the uptake of siRNA-QDs was monitored by fluorescence imaging [116]. Compared to QDs, the C-dots show advantages of better biocompatibility, lower cost, and easier preparation and are considered as a potential alternative to QDs [117]. The C-dots surface coated with alkyl–PEI2k could effectively deliver siRNA and transfect against firefly luciferase (fLuc) with inhibited expression of luciferase gene in 4 T1-luc cells, while maintaining their biocompatibility and fluorescence properties [118]. The UCNPs have gained increasing attention in recent years as a new generation of biological luminescent nanoprobes for cell labeling and optical imaging. It offers many advantages, such as deep penetration, low background autofluorescence, and high resistance to photo-bleaching, thus providing a promising optical imaging way for monitoring the siRNA transfection [119,120].

In contrast to fluorescence imaging, BLI does not require an external light illumination on the living subjects because the bioluminescence is produced by oxidation reaction of luciferin with catalytic assistance of luciferase enzyme in the body. Various luciferase genes can be introduced into biological systems *via* transfection techniques and expressed with corresponding luciferase enzymes (Fig. 5a). In this technique, there is no interference from autofluorescence and endogenous bioluminescence. Thus, BLI can provide a higher signal sensitivity and better signal-to-noise ratio than fluorescence imaging. By exposing RNAi therapeutics to cancer cells or injecting to tumor-bearing animals, the expression of bioluminescent reporters and fluorescent proteins, such as luciferases, the green fluorescent protein (GFP), and red fluorescent protein (RFP) [121], could be tested to evaluate the gene-silencing efficacy of those products. This could be helpful in forecasting their interfering ability for screening the most effective siRNA therapeutics and the best formulations before further test in human. In one study, Kay's group demonstrated the feasibility of monitoring siRNA delivery and assessing silencing effect by *in vivo* BLI (Fig. 5b, c) [122]. In another study, by co-injection of luciferase plasmid and synthetic luciferase siRNA, the silencing effect in a variety of organs was monitored through BLI [123]. Moreover, BLI was applied to assess the silencing of the activity of P-glycoprotein (Pgp), a multidrug resistance (MDR1) gene product overexpressed in multidrug-resistant cancer cells by using short hairpin RNA interference (shRNAi) [124]. The shRNAi-mediated downregulation of Pgp activity at cellular level or in animal models could be directly traced by BLI of Renilla luciferase (rLuc) reporter through its substrate, coelenterazine, which is also a known as substrate for Pgp transportation. Furthermore, the *in vivo* gene-silencing activity of luciferase siRNAs incorporated in calcium phosphate (CaP) nanoparticles was tested in a fLuc-expressing human cervical cancer cell line (HeLa-Luc). These nanoparticles were tested in transgenic mice (FVB/NJc1 female mice) with spontaneous pancreatic tumors by measuring the bioluminescence intensity with IVIS® after intraperitoneal injection of luciferin [125]. Recently, the kinetics of siRNA-mediated gene silencing combined with BLI was studied for the assessment of the best approach for gene silencing [126], for simulating/predicting the effective siRNA

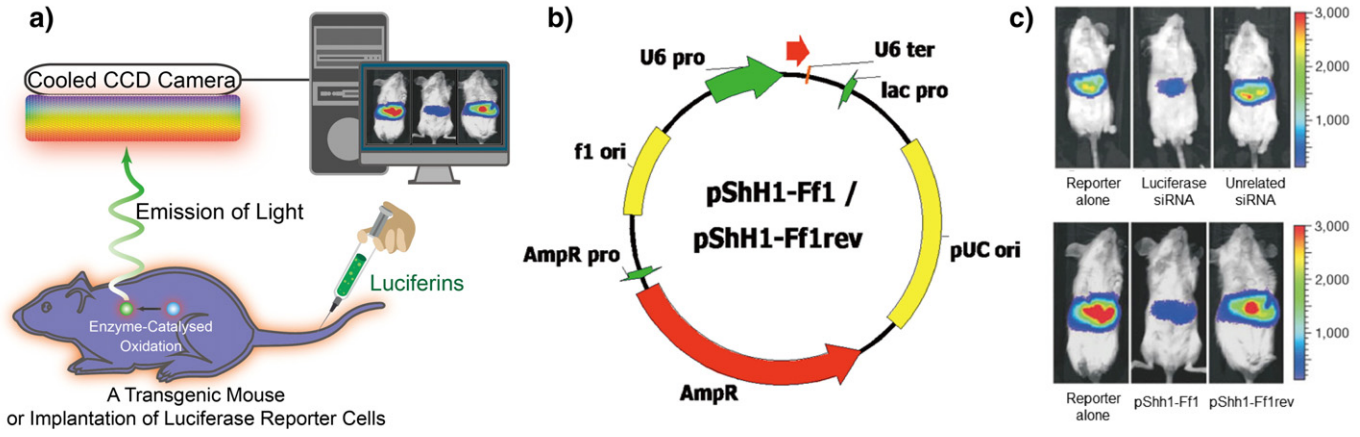

Fig. 5. Optical bioluminescence imaging. (a) A schematic illustration of the basic principle of *in vivo* bioluminescence imaging. In this case, mouse with luciferase (Luc)-labeled cancer cells that express luciferase is required. After injecting the enzyme substrate luciferin into the mouse body, the bioluminescence light is generated when the luciferin molecules interact with luciferase *via* enzyme-catalyzed oxidation. Finally, the emitted light is detected by a cooled CCD camera and the image is produced by computer. (b) The plasmids used for transfection into mouse liver. (c) Representative images (upper image) of mice co-transfected with luciferase plasmid pGL3-control without siRNA, with luciferase siRNA or with unrelated siRNA. The results indicate that the luciferase expression was specifically suppressed by siRNA-mediated inhibition in adult mice, but the unrelated siRNAs had no effect. Another result from (c) (lower image) shows the gene silencing of luciferase expression by functional shRNAs (pShh1-Ff1). These outcomes demonstrated that the plasmid-encoded shRNAs can induce an effective and specific RNAi response *in vivo*. Adapted with permission from [122].

dose based on luciferase knockdown *in vitro*, and for studying the kinetics of luciferase knockdown by RNAi therapeutics in subcutaneous tumors and their effects.

GFP and its derivatives have also been widely utilized for imaging *in vitro* gene silencing of siRNA in numerous studies [127,128]. For instance, silica-gold nanoshells were covalently decorated with epilayer of poly(L-lysine) peptide (PLL) on the surface to load single-stranded antisense DNA oligonucleotides or double-stranded short-interfering RNA (siRNA) molecules with NIR laser irradiation-triggered release of gene segments and endosomal escape [128]. The gene-silencing efficacy was evaluated by measuring the downregulation of GFP in human lung cancer H1299 GFP/RFP cell line. Cancer cells and tumor-bearing animals were used to study the gene-silencing effects for screening the RNAi products and serve as a real-time tool to investigate the efficacy of siRNA delivery in preclinical studies. Understandably, the application of these technologies in humans is limited because of need of reporter gene transfection.

4.2. PET and SPECT

PET and SPECT are nuclear imaging techniques that use radioactive tracers and detect gamma rays to provide information of molecular signatures at molecular level within living subjects (Fig. 6). Both imaging systems could afford excellent penetration depth in tissues and high sensitivity for whole-body imaging. For PET imaging, the specifically radiolabeled imaging agents are required for targeting and visualizing organs or tissues of interest. Imaging of radioactive tracer is achieved by detecting the high-energy photons (gamma ray) emitted from the radioactive isotopes during the spontaneous radioactive decay. More specifically, the nucleus of specific radioactive isotope undergoes a beta plus (β^+) decay due to its unstable nuclear system, while an excessive proton is converted into a neutron, a positron, and an electron neutrino [129]. Based on electron-positron annihilation, the collision between electron and positron produces two gamma ray photons, traveling at opposite directions at approximately 180° from each other [130,131]. The gamma ray has ten times higher energy than X-ray, and large number of emitted paired photons from radioactive isotopes detected by gamma cameras provide angular and radial distance information from regional interest [131]. These features enable high signal sensitivity and reconstruction of quantitative tomographic images.

Owing to their highly quantitative and sensitive nature, radionuclide imaging techniques have been utilized for analyzing the pharmacokinetics and biodistribution of RNAi therapeutics [132]. Relatively short half-lived isotopes such as ^{18}F ($t_{1/2}$ = 109.8 min) and ^{64}Cu ($t_{1/2}$ = 12.7 h) are frequently used as radioactive tracers to label siRNA molecules or drug delivery systems for PET imaging. In one recent study, core/shell-structured hollow gold nanospheres (HAuNS) were developed as a targeted NIR light-inducible delivery system for nuclear factor kappa-light-chain-enhancer of activated B cells (NF-κB) targeting siRNA [133]. By conjugating 1,4,7,10-tetraazacyclododecane-1,4,7,10-tetraacetic acid (DOTA) derivatives to the surface of nanospheres and labeling with ^{64}Cu, the HAuNS were applied for micro-PET/computed tomography (CT) imaging. The PET/CT images indicated that targeted HAuNS showed higher accumulation in tumors than nontargeted nanocarriers in HeLa cervical cancer bearing nude mice after intravenous injection (Fig. 7). ^{18}F-labeled siRNA has also been investigated using PET to measure the pharmacokinetics and biodistribution of siRNA delivery systems [134]. For example, Oku et al. used *N*-succinimidyl 4-^{18}F-fluorobenzoate (^{18}F-SFB) to label siRNA for real-time analysis of siRNA delivery [135]. PET images revealed that naked ^{18}F-labeled siRNA was cleared quite rapidly from the blood stream and excreted from the kidneys. However, the cationic liposome/^{18}F-labeled siRNA complexes tended to accumulate in the lung. There is an urgent need to develop facile and efficient ^{18}F-labeling methods for PET imaging of RNAi because most traditional ^{18}F-labeling strategies are time-consuming with low yield.

Single-photon emission computed tomography (SPECT) is similar to PET by utilizing radioactive materials that decay through the emission of single gamma rays (Fig. 6). By comparison, SPECT scans are significantly less expensive than PET since the cyclotron is not required to generate short half-life radioisotopes [136]. SPECT uses isotopes with longer half-lives or from generator elution, such as ^{111}In ($t_{1/2}$ = 2.8 days), ^{99m}Tc ($t_{1/2}$ = 6 h), ^{123}I ($t_{1/2}$ = 13.3 h), and ^{131}I ($t_{1/2}$ = 8 days), to provide information about localized function in internal organs with view of the distribution of radionuclides. However, as the emission of gamma rays cannot provide sufficient spatial information for tomographic reconstruction, a special instrumental design for data acquisition is required, and the sensitivity of SPECT can be over 1 order of magnitude lower than PET [136]. In a recent study, siRNA was modified with hydrazinonicotinamide (HYNIC), a chelator for technetium-99 m

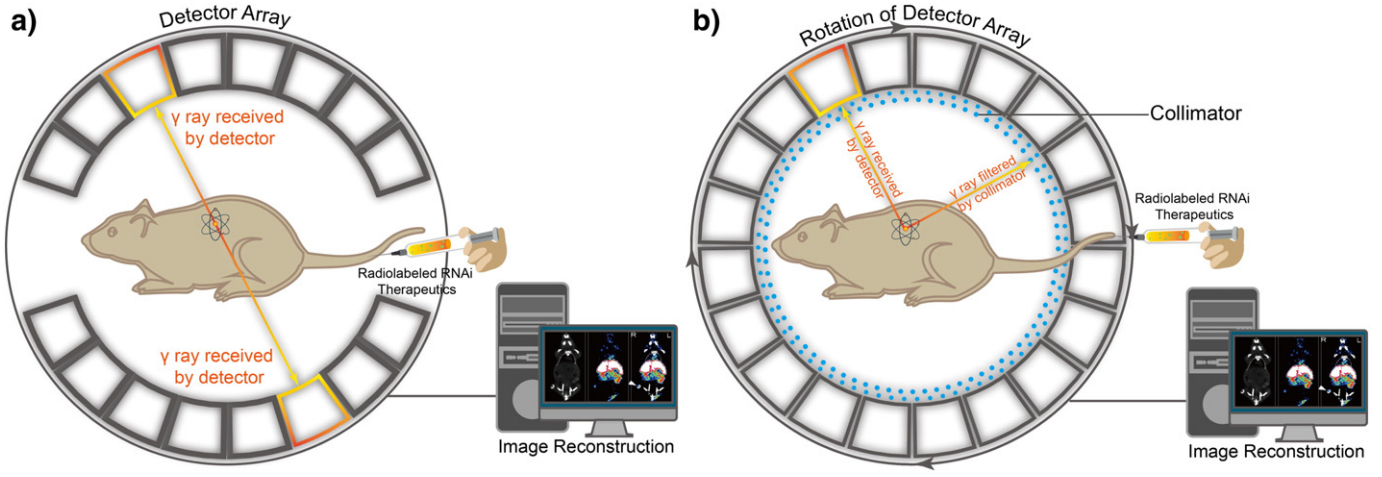

Fig. 6. Positron emission tomography (PET) and single-photon emission computed tomography (SPECT). (a) A schematic illustration of the basic principles of *in vivo* PET imaging. In this technique, the radioactive isotope-labeled RNAi therapeutics is injected into animals. Positrons are emitted from the isotopes associating with electrons, which cause annihilation and subsequent production of two gamma (γ) rays. The two high-energy γ rays are traveling at 180° from each other. Then the γ rays are received by detector array with electrical signals and finally converted into tomographic images. (b) Another schematic illustration of the basic principle of *in vivo* SPECT imaging. First, the radioactive isotopes-labeled RNAi therapeutics is administered into the mouse to emit γ rays. The γ rays produced by isotopes in SPECT do not travel in opposite directions, instead, are collected by detector array that rotates around animals, while any diagonally incident γ rays are filtered by collimator. The γ rays received by detector array are converted and reconstructed into tomographic images.

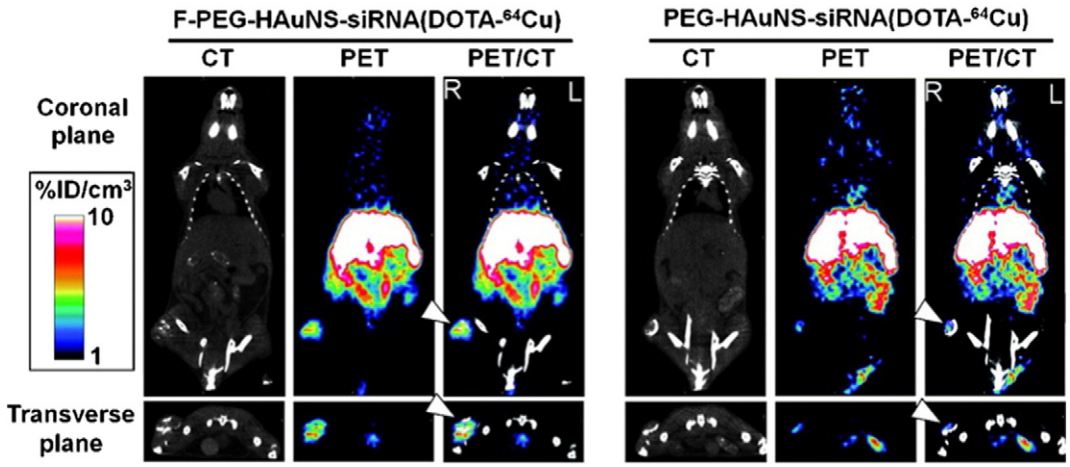

Fig. 7. Micro-PET/CT images of nude mice bearing with HeLa cervical tumor xenografts in the right rear leg at 6 h after intravenous injection of folic acid (F-PEG-HAuNS-siRNA(DOTA-^{64}Cu) or PEG-HAuNS-siRNA(DOTA-^{64}Cu). Tumors were marked by arrowheads. Figure adapted with permission from [133].

(^{99m}Tc), to monitor siRNA at cellular level by gamma counting and microautoradiography [137]. Besides, the delivery process and biodistribution in tumor-bearing mice were assessed by whole-body imaging. Merkel et al. also employed SPECT to monitor the biodistribution and pharmacokinetics of siRNA labeled with a gamma emitter (e.g., ^{111}In/^{99m}Tc) [138]. In the real-time perfusion investigation, rapid accumulation of gamma emitter-labeled siRNA in the liver and kidneys could be observed, followed by an increasing signal in the bladder. Quantification of scintillation counts in the regions of interest (ROI) revealed that the half-life of siRNA complexes in the blood pool is less than 3 min, suggesting a very rapid excretion into the bladder. Once the siRNA is labeled with radioactive probes, it can be used in non-invasive perfusion, kinetics, and biodistribution evaluation. This offers the advantage of real-time live imaging and investigation at various time points in the same animal to reduce the number of animals needed compared to conventional methods.

4.3. MRI

MRI is an important versatile technique that provides noninvasive imaging based on the principle of nuclear magnetic resonance (NMR), by using strong magnetic field and radiofrequency (RF) pulses to generate RF signal (relying on intrinsic physiological feature) for visualization (Fig. 8a). Specifically, an atom nucleus consists of a number of protons and neutrons, each of which has a constant spin and produces angular momentum, which consequently leads to a net angular momentum in the nucleus. If there is an equal number of protons and neutrons in nucleus, net angular momentum is zero. If there is an unequal number of protons and neutrons, then the nucleus gives a specific net spin angular momentum. In the latter circumstances, the nuclear Larmor precession is gained when an external magnetic field is present, and the resonant absorption of RF pulses by nucleus will occur when the frequency of RF pulses equals to the Larmor precession rate. Finally, the RF signal is generated after the removal of external magnetic field [139]. In this regard, the ^{1}H nucleus is particularly useful for MRI since it is abundant in aqueous physiological environment and is magnetically active to give a large magnetic moment to generate RF. However, the RF signal can only be detected from an excess of nuclei with spins aligned either parallel or anti-parallel direction, an equal number of nuclei spins pointing in opposite direction cannot generate detectable MR signals [129]. Therefore, MRI is limited by low sensitivity with long signal acquisition time. Nonetheless, MRI has a number of unique advantages including high spatial resolution, deep tissue penetration, and excellent soft tissue contrast. MRI has been widely used in the clinic to study the anatomy as well as function of tissues. In addition to the development of high field scanners, the design of contrast agents (CAs) plays an important role

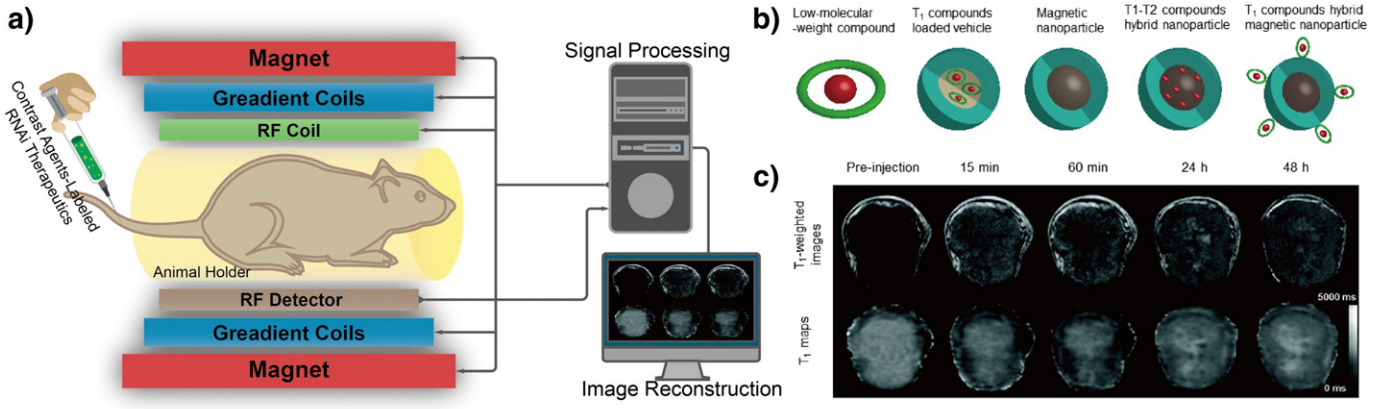

Fig. 8. Magnetic resonance imaging (MRI). (a) A schematic illustration of the basic principle of *in vivo* MR imaging. In general, an MRI scanner consists of three types of coils: the first coil provides a strong homogenous magnetic field, the second coil generates the varying strength of magnetic field in X, Y, and Z directions to encode the spatial position of MR signal and the third coil produces the radio frequency to alter the magnetic dipoles of protons in the subject, generating MR signals to be detected and reconstructed into MR image by computer. MR contrast agents can be labeled onto RNAi therapeutics to track their distribution *in vivo* through T_1 and T_2 signal enhancement. (b) Typical contrast agents for MRI, including low-molecular-weight paramagnetic compound, T_1 CA-loaded vehicle, magnetic nanoparticle, T_1-T_2 compounds hybrid nanoparticle, and T_1 compounds hybrid magnetic nanoparticle. (c) Representative T_1-weighted MR images (top) and quantitative T_1 maps (down) of a tumor (400 mm^3) before and after intravenous injection of siRNA-incorporated nanoplex at the dose of 300 mg/kg. Figures adapted with permission from [143].

to improve the image quality by enhancing the contrast of diseased regions while sparing normal tissues. Generally, the CAs could be classified as T_1 and T_2 CAs due to their magnetic properties and relaxation mechanisms (Fig. 8b).

Superparamagnetic iron oxide nanoparticles (SPIONs) have the ability to decrease the spin–spin relaxation time for T_2-weighted imaging of specific tissues. There are several types of SPIONs approved as contrast agents for MRI in the clinic [140]. Recently, Mok et al. designed and synthesized a pH-sensitive siRNA-loaded nanovector based on SPIONs. The SPIONs were modified with PEI, a commonly used gene transfection macromolecule, through acid-cleavable citraconic anhydride bonds, and coated with anti-GFP siRNA and tumor-specific ligand, chlorotoxin (CTX) [141]. The nanovectors exhibited excellent magnetic property for MRI with a significantly higher r_2 (673 mM^{-1} s^{-1}) than the commercial available T_2 contrast agents (*e.g.*, Feridex). More interestingly, the nanovectors did not elicit obvious cytotoxicity at pH 7.4, but exhibited significant cytotoxicity at pH 6.2 as a result of acidic environment-elicited cytotoxicity, which may be caused by the protonation of the primary amine at low pH. Meanwhile, the gene-silencing effect under acidic pH condition was significantly higher than that under physiological pH condition, because the surface of nanoparticles was nearly 3 times more negatively charged at pH 7.4 than that at pH 6.2. In another study, the formulation of polyethylene glycol-graft-polyethylenimine (PEG-g-PEI)-coated SPIONs were prepared, which was further modified with neuroblastoma cell specific disialoganglioside GD2 single-chain antibody fragment [142]. The nanocarriers could deliver Bcl-2 siRNA to cancer cells and knock down the expression of Bcl-2 mRNA. In addition, effective delivery of siRNA was confirmed through the *in vitro* and *in vivo* MR imaging studies.

Besides T_2 CAs, paramagnetic compounds, such as gadolinium and manganese-based compounds, can elevate the relaxation potential by reducing the T_1 relaxation time, which are widely applied as T_1 contrast agents. Recently, a type of nanoplex that self-assembled from fluorescein isothiocyanate (FITC)-labeled siRNA-chk duplexes and rhodamine-labeled PEI, in which the PEI segments was linked to poly-L-lysine (PLL) with dual-labeling of Cy5.5 and Gd-DOTA, while the PLL-end was combined with prodrug enzyme bacterial cytosine deaminase (bCD) that can convert the nontoxic prodrug 5-fluorocytosine (5-FC) to cytotoxic 5-fluorouracil (5-FU), for imaging-guided RNAi cancer therapy [143]. The nanoplex labeled with different types of CAs could make it possible for MR and optical imaging of the delivery of siRNA and the function of prodrug enzyme in breast tumors for image-guided and molecular targeted cancer therapy. For instance, the high-resolution T_1-weighted MR images and quantitative T_1 map of tumor region were obtained by MRI, and the contrast in tumor region was enhanced after the administration of nanoplex (Fig. 8c) with T_1 value change as a result of the accumulation and diffusion of the nanoplex, demonstrating successful delivery of siRNA into tumor tissues also confirmed by optical imaging. The delivered siRNA could downregulate the activity of aggressive enzyme of choline kinase-α (Chk-α) in breast cancer cells, while the bCD could convert 5-FC to 5-FU, which procedure could be noninvasively monitored by ^{1}H MR spectroscopic imaging and ^{19}F MR spectroscopy. In another study, hollow manganese oxide nanoparticles (HMONs) were exploited as a theranostic nanoplatform for simultaneous cancer targeted siRNA delivery and MR imaging [144]. In this study, HMON nanoparticles were coupled with 3,4-dihydroxy-L-phenylalanine conjugated branched PEI (PEI-DOPA) through the strong affinity between DOPA and metal oxides and further modified with Herceptin, a therapeutic monoclonal antibody to target Her-2 expressing cancer cells selectively. Although SPIONs have already been widely used as T_2 MRI contrast agents, they still have some drawbacks, such as magnetic susceptibility artifacts and negative contrast, which limit their clinical applications [145]. The development of T_1-T_2 dual-modal contrast agents has attracted considerable interest because they can provide the contrast for T_1-weighted imaging with high tissue resolution and for T_2-weighted imaging with high feasibility of lesions detection. Recently, Wang et al. reported a low-molecular-weight polyethylenimine (stPEI)-wrapped and gadolinium-embedded iron oxide (GdIO) nanoclusters (GdIO–stPEI) for T_1–T_2 dual-modal MRI-visible siRNA delivery, which exhibited high relaxivities for MRI measurements and suppressed expression of luciferase proteins for dual-type of MR imaging-guided siRNA delivery [146].

4.4. Ultrasound

Ultrasound is a clinically widely equipped imaging modality for evaluating the structure, function, and blood flow of organs, which could provide images with high spatial and temporal resolution at low cost (Fig. 9a). Ultrasound scanners can emit sound waves with frequencies between 1 and 20 MHz and receive feedback waves reflected by tissues based on density difference to build images for diagnosis [147], which could provide images in a real-time manner without processing delay after acquisition compared with other imaging modalities [40]. In principle, the signal reflected from tissues is insufficient for precise diagnosis because of artifacts from normal tissues. Thus, ultrasound contrast agents are essential to increase the imaging accuracy. Some contrast agents have been developed to enhance positive signal for ultrasound imaging [148–150], such as microbubbles [151–153], nanodroplets [154–157], nanobubbles [158,159], and liposomes [160,161] (Fig. 9b). These are usually constructed with shell of proteins, polymers, lipids, or surfactants to maintain stability in the bloodstream as well as escaping from RES, while loading air or biologically inert heavy gas such as nitrogen, perfluorocarbons, and sulfur hexafluoride to generate echogenicity (Fig. 9b) [162]. Besides, solid nanoparticles with cavities

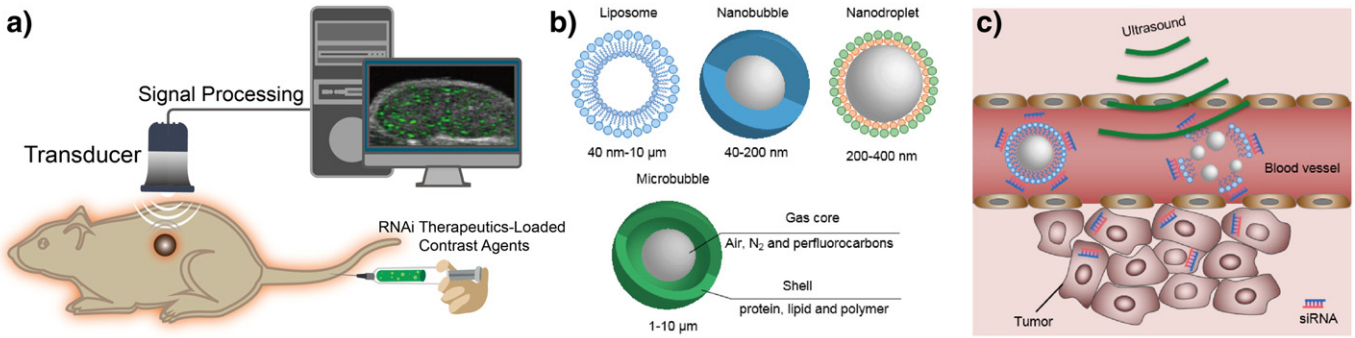

Fig. 9. Ultrasound imaging. (a) A schematic illustration of the basic principle of *in vivo* ultrasound imaging. First, the ultrasound contrast agent that encapsulates RNAi therapeutics is injected into animals, then high-frequency sound waves are sent and penetrated into the subjects, while the time intervals of subsequent reflection of sound waves is recorded by a transducer. The detected signals are converted and constructed into images. A coupling medium is usually used between the contact surface of transducer and subject for sound wave transmission. (b) Typical contrast agents for ultrasound, such as liposome, nanobubble, nanodroplet, and microbubble. (c) Ultrasound-triggered destruction of siRNA-incorporated microbubbles. Ultrasound could disrupt the contrast agents with high acoustic pressure to release RNAi agents when delivered to the blood vessels of the tumor region. Then the released RNAi agents enter into tumor cells to silence target gene.

that can trap gas [163], and nanoparticles constructed with gas generating materials have also been applied to enhance the contrast for ultrasound imaging [164].

Ultrasound demonstrates potential advantages in the development of RNAi therapeutics. First, with low acoustic pressure (<100 kPa) when the ultrasound probe arrives the tumor vasculature, ultrasound could be used to diagnose tumors for imaging-guided delivery of RNAi therapeutics and monitoring the therapeutic effects. Besides, by applying high acoustic pressure (100 kPa to several MPa), ultrasound could be applied to disrupt the probes to release cargos (drugs or RNAs) in target positions and change the permeability of cell membrane with more siRNA delivered intracellularly for gene silencing [152]. As a result, ultrasound can enhance therapeutic effect of RNAi therapeutics (Fig. 9c) [149,165]. The siRNA molecules can be attached to the surface of microbubbles or trapped in the bilayer of liposomes, or siRNA-loaded nanoparticles can be incorporated into ultrasound probes. For instance, epidermal growth factor receptor (EGFR)-directed siRNA (EGFR-siRNA) could be efficiently attached to microbubbles with around 7 mg siRNA per 10^9 microbubbles and safely protect siRNA from RNase digestion [166]. The EGFR-siRNA-loaded microbubbles reduced the EGFR expression of murine squamous carcinoma cells *in vitro*, and the ultrasound-triggered destruction of microbubbles released EGFR-siRNA specifically in the tumor region to effectively delayed tumor growth, while the tumor volume was monitored by ultrasound.

However, microbubbles are limited to vascular compartment with poor tumor tissue penetration because of its large size and relatively poor stability. Therefore, ultrasound probes with much smaller size, such as nanobubbles, nanoparticles, and nanoscale liposomes, with better tumor tissue penetration properties have been fabricated for ultrasound diagnosis and ultrasound-mediated siRNA delivery with better tumor accumulation [157,167]. For instance, the ultrasound-sensitive siRNA nanobubbles made from positively charged liposomes with gas core and decorated with negatively charged siRNAs on the surface could effectively accumulate in the tumor tissues through EPR effect, demonstrating high potency for tumor imaging and targeted delivery of siRNA for RNAi therapy [168]. Moreover, high cellular affinity ligands have been introduced to the surface of ultrasound nanoprobes, such as aptamer-decorated nanobubbles have been developed to specifically target the CCRF-CEM cells (T-cells, human acute lymphoblastic leukemia) for ultrasound imaging [159]. Other bioactive compounds, such as anticancer drugs and plasmid DNA, could also be co-loaded into probes for ultrasound imaging and combination therapy of tumors [160].

4.5. Multimodality imaging

Although each imaging modality has its unique advantages, it is also endowed with its intrinsic limitations making it difficult to obtain accurate and reliable information on all aspects of structure and function about the target organs by a single imaging modality [169]. Table 2 summarizes some general features of classical imaging modalities including optical imaging, radionuclide imaging, MRI, and ultrasound imaging. To cope with the shortcomings of each modality, multimodality imaging combines different imaging techniques and imaging probes and can provide some complementary information about RNAi therapeutics. However, in context of developing multimodality probes, it should be noted that challenges are involved especially for applications in living subjects. Since the multimodality probes are primarily nanoparticle based, such as organic dye-labeled iron oxides, gadolinium chelates functionalized QDs, magnetic microbubbles, radiolabeled C-dots, etc. The major problems may be associated with insufficient concentration of probes at target sites due to the undesired uptake by mononuclear

Table 2
Features of different modalities for structural, functional, and molecular imaging of RNAi.

Modality	Penetration depth	Sensitivity (Mol/L)	Spatial resolution	Physical medium	Imaging probes and amount of use		Advantages	Disadvantages
Optical FI	<1 cm	~10^{-9}–10^{-12}	2–3 mm	Visible or NIR light	Organic dyes; QDs; C-dots; UCNPs	Microgram–milligram	High sensitivity; real-time imaging; nonionizing radiation; relatively inexpensive; short acquisition time; multiplexing capability	Low spatial resolution at greater depth; limited penetration depth; autofluorescence
Optical BLI	< 2 cm	~10^{-15}–10^{-17}	3–5 mm	Visible light	GFP; RFP	Microgram–milligram	High sensitivity; real-time imaging; no ionizing radiation; relatively inexpensive; short acquisition time; user friendly; multiplexing capability	Low spatial resolution at greater depth; Limited penetration depth; genetic reporter systems required
PET	Limitless	~10^{-11}–10^{-12}	1–2 mm	High-energy γ-rays	Radiolabeled tracers	Nanograms	Excellent sensitivity; limitless penetration depth; quantitative data	High cost of cyclotron; Ionizing radiation; limited spatial resolution
SPECT	Limitless	10^{-10}–10^{-11}	1–2 mm	Low-energy γ-rays	Radiolabeled tracers	Nanogram	Excellent sensitivity; limitless penetration depth; no need of cyclotron; multiplexing capability	Relatively expensive; ionizing radiation; limited spatial resolution; semi-quantitative
MRI	Limitless	10^{-3}–10^{-5}	~1 mm	Radio waves	Gadolinium chelates; Iron oxides; Other magnetic nanoparticles	Microgram–milligram	Excellent spatial resolution; limitless penetration depth; quantitative data; no ionizing radiation	Relatively expensive; relatively low sensitivity and poor contrast; long acquisition time
US	Millimeters–centimeters (frequency dependent)	—	0.01–2 mm	Ultrasound waves	Microbubbles	Microgram–milligram	Relatively inexpensive; no ionizing radiation; quantitative data; no ionizing radiation; short acquisition time; high sensitivity with microbubbles	Limited penetration depth; poor low contrast; strong boundary effect; limited to imaging soft tissue only

BLI: bioluminescence imaging; FI: fluorescence imaging; US: ultrasound; NIR: near-infrared fluorescence; GFP: green fluorescent protein; RFP: red fluorescent protein; QDs: quantum dots; C-dots: Carbon nanodots; UCNPs: upconvertion nanoparticles.

phagocyte system (MPS). Other concerns include slow clearance time, long-term retention in tissues and organs, as well as the long-term toxicity. These issues are highly related to the physicochemical properties (e.g., chemical component, size distribution, final hydrodynamic diameter, shape, surface charge) of nanoprobes [170]. In addition, different modalities differ in their imaging sensitivity by large magnitude [171]. Thus, the combination of two different probes needs to be carefully designed with proper ratio [172]. Therefore, in order to reach the full potential of multimodality imaging, the participations of multidisciplinary scientists with solid background in nanotechnology, material science, pharmacology, pharmaceutical chemistry, clinical medicine, biomedical engineering, and instrumental techniques are essential in the early development stages [173,174].

A typical example of a multimodality probe-siRNA delivery system for *in vivo* imaging of RNAi has been reported by Medarova et al. [175]. In this study, a dual-purpose probe was developed, which was composed of iron oxide core and Cy5.5 dye on the surface. The probe was further modified with cell membrane translocation peptides to facilitate intracellular delivery of siRNA (Fig. 10a). The successful delivery of GFP siRNA duplex to tumors was assessed by MRI and optical imaging of tumor-bearing animals after intravenous injection of the probes (Fig. 10b,c). In another study, both commercial MRI contrast agents (Magnevist/Feridex) and Alexa-647 dye-labeled siRNA for targeting cyclooxygenase-2 (COX-2), an important therapeutic target in cancer, were encapsulated in PEGylated polycationic liposomes. The liposomes were used to assess the delivery and silencing effects of siRNA *in vivo* [176]. It was found that Feridex-loaded liposomes demonstrated better performance than that of Magnevist, which was further tested *in vivo*. Both MRI and optical imaging confirmed successful delivery of siRNA to MDA-MB-231 tumor.

Recently, PET/CT combined with BLI was also employed to monitor the whole-body biodistribution of RNAi therapeutics and assess their silencing effects of the expression of luciferase *in vivo* [177]. The nanoparticles were prepared with cyclodextrin-containing polycations and anti-Luc siRNAs with their 5′-end conjugated with 1,4,7,10-tetraazacyclododecane-1,4,7,10-tetraaceticacid (DOTA) for ^{64}Cu labeling. Micro-PET/CT was carried out to determine the distribution and tumor accumulation of siRNA-containing nanoparticles. No obvious difference in distribution between the targeted nanoparticles and nontargeted ones was observed. Meanwhile, the BLI revealed that the targeted nanoparticles had better RNAi effects 1 day after injection, demonstrating the importance of multimodal imaging. Thus, the combination of PET/CT and BLI is important to simultaneously monitor both the gene delivery and silencing effects of RNAi, which is critical for the design of RNAi therapeutics for clinical translation.

5. Conclusions and perspectives

This review summarized the application of various imaging modalities for qualitative and quantitative assessments of RNAi therapeutics to promote their applications in cancer therapy and translate them into clinical applications. Overall, a variety of RNAi therapeutics have been developed and some of them are under clinical evaluation. Diverse imaging techniques have been applied to study the mechanism of gene transfection, route of delivery, systemic distribution in the body, gene-silencing effect, and therapeutic outcomes.

RNAi has demonstrated great potential for treating a wide range of diseases, especially for multidrug-resistant cancer treatment, which are difficult to be treated by conventional methods of chemotherapy and radiotherapy. Despite the positive progresses in translating some RNAi formulations into clinical trial for cancer therapy, several issues are required to bear in mind for effective translation of RNAi therapeutics from bench to bedside: (1) How to optimize the parameters/conditions to accumulate sufficient amount of RNAi therapeutics in tumor tissues and translocate them into cancer cells; (2) How to select the proper target to maximize the therapeutic effects of siRNA; and (3) How to develop new effective gene carriers with high stability during circulation as well as controlled release function of payload nucleic acids inside cancer cells with high gene transfection effects. Finally, the ideal RNAi formulations should satisfy the requirement of specific delivery of RNAi agents to tumors and efficiently transfer into cancer cells to silence target genes at high performance for tumor suppression, while avoiding potential toxicity, side effects, and off-target silencing.

The advances in noninvasive imaging techniques provide new approaches to visualize and quantify RNAi in cancer therapy and further understand the mechanism of RNAi intracellular and in the body. So far, several imaging modalities, such as optical imaging, MRI, ultrasound, and SPECT/PET, have been applied to assess the delivery of siRNA, to determine the biodistribution, and to monitor the therapeutic effects, leading to a significant contribution to the progresses of RNAi therapeutics, especially in the preclinical studies [178]. It is very important to establish proper evaluation models/systems with the aid of molecular imaging in preclinical studies and translate the animal results as important references for clinical trial in human. As each imaging

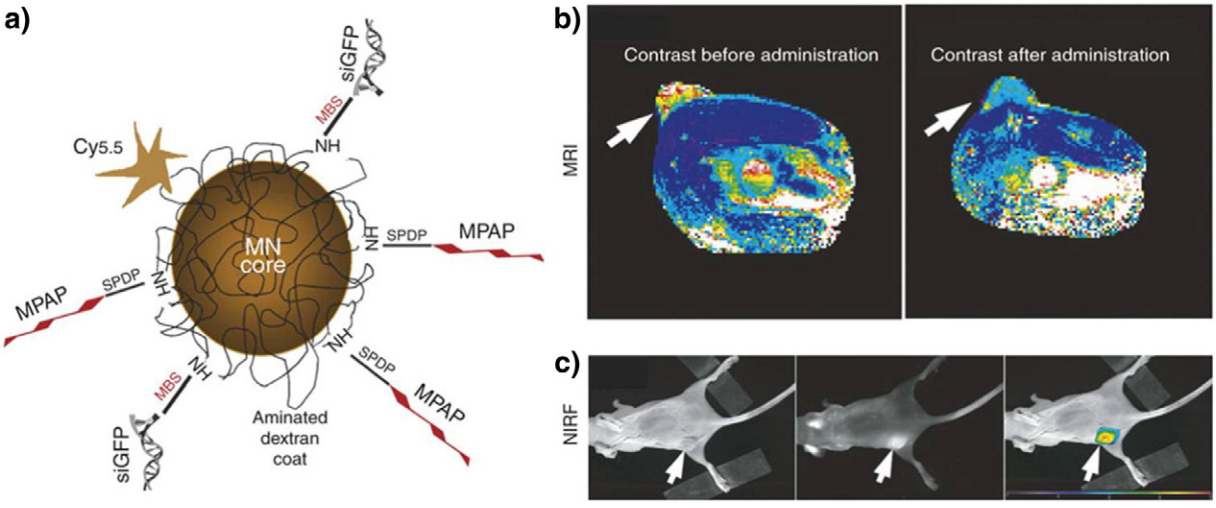

Fig. 10. Multimodality *in vivo* imaging of RNAi by using MRI and optical imaging. (a) Schematic illustration of the multifunctional nanocarriers with core of magnetic nanoparticles, and surface conjugated with Cy5.5, GFP siRNA (siGFP), and membrane translocation peptides (MPAP). (b) *In vivo* MR imaging of mice bearing with subcutaneous LS174T human colorectal adenocarcinoma tumors (arrows) before and after the administration of the multifunctional nanocarriers, indicating significant drop of T_2-weighted contrast enhancement in tumor regions after injection of the contrast agents. (c) A high-intensity NIRF signal in the tumor confirmed the successful delivery of the nanocarriers, while the left mouse with white light, middle one with NIRF, and right one with color-coded overlay. Adapted with permission from [175].

modality has its intrinsic advantages and limitations, there is a trend to combine different imaging modalities for better tracing the fate of siRNA, the delivery vehicles, and the therapeutic effects, which is expected to maximize the potential of cancer therapy with RNAi therapeutics and help overcome the barriers that block the road to clinical translation.

The rational design of molecular imaging probes is essential to accurately monitor the biological processes of RNAi therapeutics and fully realize their potency in cancer therapy. Molecular imaging probes for RNAi-based cancer therapeutics, consisting of a variety of functional nanomaterials including lipids, metals, carbons, polymers, and biologics-based nanoparticles, should be relatively safe for clinical use with low toxicity and biodegradability in the body. Further development of new imaging contrast agents, which can increase the signal intensity for more reliable image analysis with cancer cell specific targeting ability, would optimize the diagnostic selectivity and provide more detailed and accurate pathological information about the biological processes of RNAi therapeutics in cancer treatment. Furthermore, the technical advances in imaging devices would enable proper patient selection and rapid translation of RNAi therapeutics into clinic.

Acknowledgments

This study was supported in part by the Major State Basic Research Development Program of China (973 Program) (grant nos. 2014CB744503 and 2013CB733802), the National Natural Science Foundation of China (NSFC) (grant nos. 81422023, 81101101, 81371596, U1505221 and 51273165), the Key Project of Chinese Ministry of Education (grant no. 212149), the Fundamental Research Funds for the Central Universities, China (grant nos. 20720160065 and 20720150141), the Program for New Century Excellent Talents in University (NCET-13-0502), the Shenzhen municipal government project no. JCYJ20130401164750006, Research of CUHK (ref. nos. 4054012 and 4054087), the focused investments scheme of CUHK (ref. no. 1902062), the Hong Kong RGC CRF (ref. no. CUHK4/CRF/12G), and the Intramural Research Program, National Institute of Biomedical Imaging and Bioengineering, National Institutes of Health.

References

[1] A. Fire, S. Xu, M.K. Montgomery, S.A. Kostas, S.E. Driver, C.C. Mello, Potent and specific genetic interference by double-stranded RNA in *Caenorhabditis elegans*, Nature 391 (1998) 806–811.
[2] S.M. Elbashir, J. Harborth, W. Lendeckel, A. Yalcin, K. Weber, T. Tuschl, Duplexes of 21-nucleotide RNAs mediate RNA interference in cultured mammalian cells, Nature 411 (2001) 494–498.
[3] S.L. Ginn, I.E. Alexander, M.L. Edelstein, M.R. Abedi, J. Wixon, Gene therapy clinical trials worldwide to 2012—an update, J. Gene Med. 15 (2013) 65–77.
[4] E.P. Thi, C.E. Mire, R. Ursic-Bedoya, J.B. Geisbert, A.C.H. Lee, K.N. Agans, M. Robbins, D.J. Deer, K.A. Fenton, I. MacLachlan, T.W. Geisbert, Marburg virus infection in nonhuman primates: therapeutic treatment by lipid-encapsulated siRNA, Sci. Transl. Med. 6 (2014) 250ra116.
[5] P.K. Kaiser, R.C. Symons, S.M. Shah, E.J. Quinlan, H. Tabandeh, D.V. Do, G. Reisen, J.A. Lockridge, B. Short, R. Guerciolini, Q.D. Nguyen, RNAi-based treatment for neovascular age-related macular degeneration by Sirna-027, Am. J. Ophthalmol. 150 (2010) 33–39, e32.
[6] R.M. O'Connell, D.S. Rao, A.A. Chaudhuri, D. Baltimore, Physiological and pathological roles for microRNAs in the immune system, Nat. Rev. Immunol. 10 (2010) 111–122.
[7] E. van Rooij, E.N. Olson, MicroRNA therapeutics for cardiovascular disease: opportunities and obstacles, Nat. Rev. Drug Discov. 11 (2012) 860–872.
[8] T. Coelho, D. Adams, A. Silva, P. Lozeron, P.N. Hawkins, T. Mant, J. Perez, J. Chiesa, S. Warrington, E. Tranter, M. Munisamy, R. Falzone, J. Harrop, J. Cehelsky, B.R. Bettencourt, M. Geissler, J.S. Butler, A. Sehgal, R.E. Meyers, Q. Chen, T. Borland, R.M. Hutabarat, V.A. Clausen, R. Alvarez, K. Fitzgerald, C. Gamba-Vitalo, S.V. Nochur, A.K. Vaishnaw, D.W. Sah, J.A. Gollob, O.B. Suhr, Safety and efficacy of RNAi therapy for transthyretin amyloidosis, N. Engl. J. Med. 369 (2013) 819–829.
[9] M.E. Davis, J.E. Zuckerman, C.H. Choi, D. Seligson, A. Tolcher, C.A. Alabi, Y. Yen, J.D. Heidel, A. Ribas, Evidence of RNAi in humans from systemically administered siRNA via targeted nanoparticles, Nature 464 (2010) 1067–1070.
[10] H. Shen, T. Sun, M. Ferrari, Nanovector delivery of siRNA for cancer therapy, Cancer Gene Ther. 19 (2012) 367–373.
[11] J. Tabernero, G.I. Shapiro, P.M. LoRusso, A. Cervantes, G.K. Schwartz, G.J. Weiss, L. Paz-Ares, D.C. Cho, J.R. Infante, M. Alsina, M.M. Gounder, R. Falzone, J. Harrop, A.C. White, I. Toudjarska, D. Bumcrot, R.E. Meyers, G. Hinkle, N. Svrzikapa, R.M. Hutabarat, V.A. Clausen, J. Cehelsky, S.V. Nochur, C. Gamba-Vitalo, A.K. Vaishnaw, D.W. Sah, J.A. Gollob, H.A. Burris 3rd, First-in-humans trial of an RNA interference therapeutic targeting VEGF and KSP in cancer patients with liver involvement, Cancer Discov. 3 (2013) 406–417.
[12] F. Alexis, E. Pridgen, L.K. Molnar, O.C. Farokhzad, Factors affecting the clearance and biodistribution of polymeric nanoparticles, Mol. Pharm. 5 (2008) 505–515.
[13] K.A. Whitehead, R. Langer, D.G. Anderson, Knocking down barriers: advances in siRNA delivery, Nat. Rev. Drug Discov. 8 (2009) 129–138.
[14] W. Li, F.C. Szoka Jr., Lipid-based nanoparticles for nucleic acid delivery, Pharm. Res. 24 (2007) 438–449.
[15] M.A. Mintzer, E.E. Simanek, Nonviral vectors for gene delivery, Chem. Rev. 109 (2009) 259–302.
[16] A. Akinc, A. Zumbuehl, M. Goldberg, E.S. Leshchiner, V. Busini, N. Hossain, S.A. Bacallado, D.N. Nguyen, J. Fuller, R. Alvarez, A. Borodovsky, T. Borland, R. Constien, A. de Fougerolles, J.R. Dorkin, K. Narayanannair Jayaprakash, M. Jayaraman, M. John, V. Koteliansky, M. Manoharan, L. Nechev, J. Qin, T. Racie, D. Raitcheva, K.G. Rajeev, D.W. Sah, J. Soutschek, I. Toudjarska, H.P. Vornlocher, T.S. Zimmermann, R. Langer, D.G. Anderson, A combinatorial library of lipid-like materials for delivery of RNAi therapeutics, Nat. Biotechnol. 26 (2008) 561–569.
[17] S.C. Semple, A. Akinc, J. Chen, A.P. Sandhu, B.L. Mui, C.K. Cho, D.W. Sah, D. Stebbing, E.J. Crosley, E. Yaworski, I.M. Hafez, J.R. Dorkin, J. Qin, K. Lam, K.G. Rajeev, K.F. Wong, L.B. Jeffs, L. Nechev, M.L. Eisenhardt, M. Jayaraman, M. Kazem, M.A. Maier, M. Srinivasulu, M.J. Weinstein, Q. Chen, R. Alvarez, S.A. Barros, S. De, S.K. Klimuk, T. Borland, V. Kosovrasti, W.L. Cantley, Y.K. Tam, M. Manoharan, M.A. Ciufolini, M.A. Tracy, A. de Fougerolles, I. MacLachlan, P.R. Cullis, T.D. Madden, M.J. Hope, Rational design of cationic lipids for siRNA delivery, Nat. Biotechnol. 28 (2010) 172–176.
[18] C.C. Lee, J.A. MacKay, J.M. Frechet, F.C. Szoka, Designing dendrimers for biological applications, Nat. Biotechnol. 23 (2005) 1517–1526.
[19] D.W. Pack, A.S. Hoffman, S. Pun, P.S. Stayton, Design and development of polymers for gene delivery, Nat. Rev. Drug Discov. 4 (2005) 581–593.
[20] M. Thomas, A.M. Klibanov, Non-viral gene therapy: polycation-mediated DNA delivery, Appl. Microbiol. Biotechnol. 62 (2003) 27–34.
[21] R.H. Mo, J.L. Zaro, W.C. Shen, Comparison of cationic and amphipathic cell penetrating peptides for siRNA delivery and efficacy, Mol. Pharm. 9 (2012) 299–309.
[22] M.E. Martin, K.G. Rice, Peptide-guided gene delivery, AAPS J. 9 (2007) E18–E29.
[23] J.P. Dassie, X.Y. Liu, G.S. Thomas, R.M. Whitaker, K.W. Thiel, K.R. Stockdale, D.K. Meyerholz, A.P. McCaffrey, J.O. McNamara 2nd, P.H. Giangrande, Systemic administration of optimized aptamer-siRNA chimeras promotes regression of PSMA-expressing tumors, Nat. Biotechnol. 27 (2009) 839–849.
[24] Y.D. Yao, T.M. Sun, S.Y. Huang, S. Dou, L. Lin, J.N. Chen, J.B. Ruan, C.Q. Mao, F.Y. Yu, M.S. Zeng, J.Y. Zang, Q. Liu, F.X. Su, P. Zhang, J. Lieberman, J. Wang, E. Song, Targeted delivery of PLK1-siRNA by ScFv suppresses Her2+ breast cancer growth and metastasis, Sci. Transl. Med. 4 (2012) 130ra148.
[25] K.Y. Choi, O.F. Silvestre, X. Huang, N. Hida, G. Liu, D.N. Ho, S. Lee, S.W. Lee, J.I. Hong, X. Chen, A nanoparticle formula for delivering siRNA or miRNAs to tumor cells in cell culture and in vivo, Nat. Protoc. 9 (2014) 1900–1915.
[26] K.Y. Choi, O.F. Silvestre, X. Huang, K.H. Min, G.P. Howard, N. Hida, A.J. Jin, N. Carvajal, S.W. Lee, J.I. Hong, X. Chen, Versatile RNA interference nanoplatform for systemic delivery of RNAs, ACS Nano 8 (2014) 4559–4570.
[27] G. Liu, K.Y. Choi, A. Bhirde, M. Swierczewska, J. Yin, S.W. Lee, J.H. Park, J.I. Hong, J. Xie, G. Niu, D.O. Kiesewetter, S. Lee, X. Chen, Sticky nanoparticles: a platform for siRNA delivery by a bis(zinc(II) dipicolylamine)-functionalized, self-assembled nanoconjugate, Angew. Chem. Int. Ed. 51 (2012) 445–449.
[28] V. Sokolova, M. Epple, Inorganic nanoparticles as carriers of nucleic acids into cells, Angew. Chem. Int. Ed. Engl. 47 (2008) 1382–1395.
[29] K.A. Afonin, M. Viard, A.Y. Koyfman, A.N. Martins, W.K. Kasprzak, M. Panigaj, R. Desai, A. Santhanam, W.W. Grabow, L. Jaeger, E. Heldman, J. Reiser, W. Chiu, E.O. Freed, B.A. Shapiro, Multifunctional RNA nanoparticles, Nano Lett. 14 (2014) 5662–5671.
[30] D.X. Cui, C.L. Zhang, B. Liu, Y. Shu, T. Du, D. Shu, K. Wang, F.P. Dai, Y.L. Liu, C. Li, F. Pan, Y.M. Yang, J. Ni, H. Li, B. Brand-Saberi, P.X. Guo, Regression of gastric cancer by systemic injection of RNA nanoparticles carrying both ligand and siRNA, Sci. Rep. 5 (2015), e10726.
[31] H. Lee, A.K.R. Lytton-Jean, Y. Chen, K.T. Love, A.I. Park, E.D. Karagiannis, A. Sehgal, W. Querbes, C.S. Zurenko, M. Jayaraman, C.G. Peng, K. Charisse, A. Borodovsky, M. Manoharan, J.S. Donahoe, J. Truelove, M. Nahrendorf, R. Langer, D.G. Anderson, Molecularly self-assembled nucleic acid nanoparticles for targeted in vivo siRNA delivery, Nat. Nanotechnol. 7 (2012) 389–393.
[32] P. Rychahou, F. Haque, Y. Shu, Y. Zaytseva, H.L. Weiss, E.Y. Lee, W. Mustain, J. Valentino, P. Guo, B.M. Evers, Delivery of RNA nanoparticles into colorectal cancer metastases following systemic administration, ACS Nano 9 (2015) 1108–1116.
[33] D. Shu, H. Li, Y. Shu, G. Xiong, W.E. Carson 3rd, F. Haque, R. Xu, P. Guo, Systemic delivery of anti-miRNA for suppression of triple negative breast cancer utilizing RNA nanotechnology, ACS Nano 9 (2015) 9731–9740.
[34] D. Haussecker, Current issues of RNAi therapeutics delivery and development, J. Control. Release 195 (2014) 49–54.
[35] J. Wang, Z. Lu, M.G. Wientjes, J.L.S. Au, Delivery of siRNA therapeutics: barriers and carriers, AAPS J. 12 (2010) 492–503.
[36] V. Hornung, M. Guenthner-Biller, C. Bourquin, A. Ablasser, M. Schlee, S. Uematsu, A. Noronha, M. Manoharan, S. Akira, A. de Fougerolles, S. Endres, G. Hartmann, Sequence-specific potent induction of IFN-alpha by short interfering RNA in plasmacytoid dendritic cells through TLR7, Nat. Med. 11 (2005) 263–270.

[37] A.D. Judge, V. Sood, J.R. Shaw, D. Fang, K. McClintock, I. MacLachlan, Sequence-dependent stimulation of the mammalian innate immune response by synthetic siRNA, Nat. Biotechnol. 23 (2005) 457–462.
[38] A.L. Jackson, J. Burchard, J. Schelter, B.N. Chau, M. Cleary, L. Lim, P.S. Linsley, Widespread siRNA "off-target" transcript silencing mediated by seed region sequence complementarity, RNA 12 (2006) 1179–1187.
[39] H. Hong, Y. Zhang, W.B. Cai, In vivo imaging of RNA Interference, J. Nucl. Med. 51 (2010) 169–172.
[40] J.K. Willmann, N. van Bruggen, L.M. Dinkelborg, S.S. Gambhir, Molecular imaging in drug development, Nat. Rev. Drug Discov. 7 (2008) 591–607.
[41] S.Y. Wu, G. Lopez-Berestein, G.A. Calin, A.K. Sood, RNAi therapies: drugging the undruggable, Sci. Transl. Med. 6 (2014) 240–247.
[42] C.H. Contag, M.H. Bachmann, Advances in in vivo bioluminescence imaging of gene expression, Annu. Rev. Biomed. Eng. 4 (2002) 235–260.
[43] F. Wang, X. Song, X. Li, J. Xin, S. Wang, W. Yang, J. Wang, K. Wu, X. Chen, J. Liang, J. Tian, F. Cao, Noninvasive visualization of microRNA-16 in the chemoresistance of gastric cancer using a dual reporter gene imaging system, PLoS ONE 8 (2013), e61792.
[44] X. Huang, S. Lee, X. Chen, Design of "smart" probes for optical imaging of apoptosis, Am. J. Nucl. Med. Mol Imaging 1 (2011) 3–17.
[45] D.E. Sosnovik, R. Weissleder, Emerging concepts in molecular MRI, Curr. Opin. Biotechnol. 18 (2007) 4–10.
[46] M.M. Alauddin, Positron emission tomography (PET) imaging with (18)F-based radiotracers, Am. J. Nucl. Med. Mol Imaging. 2 (2012) 55–76.
[47] P. Bhargava, G. He, A. Samarghandi, E.S. Delpassand, Pictorial review of SPECT/CT imaging applications in clinical nuclear medicine, Am. J. Nucl. Med. Mol Imaging. 2 (2012) 221–231.
[48] P.A. Dayton, J.J. Rychak, Molecular ultrasound imaging using microbubble contrast agents, Front. Biosci. 12 (2007) 5124–5142.
[49] S.I. Pai, Y.Y. Lin, B. Macaes, A. Meneshian, C.F. Hung, T.C. Wu, Prospects of RNA interference therapy for cancer, Gene Ther. 13 (2006) 464–477.
[50] D.D. Rao, Z.H. Wang, N. Senzer, J. Nemunaitis, RNA Interference and personalized cancer therapy, Discov. Med. 81 (2013) 101–110.
[51] M.D.A.C. Center, EphA2 Gene Targeting Using Neutral Liposomal Small Interfering RNA Delivery (IND# 72924): A Phase I Clinical Trial, https://clinicaltrials.gov/ct2/show/NCT01591356?term=NCT015913562012.
[52] C.C.C.o.W.F. University, A Phase 1, Open-Label, Dose-Ranging Study to Assess the Safety and Immunologic Activity of APN401, https://clinicaltrials.gov/ct2/show/NCT021662552014.
[53] S. Pruitt, Phase I Study of Active Immunotherapy of Metastatic Melanoma with Mature Autologous Dendritic Cells Transfected with Tumor Antigen RNA and Small Inhibitory RNAs to Alter Proteasomal Antigen Processing, https://clinicaltrials.gov/ct2/show/NCT006725422008.
[54] S.T. GmbH, A Prospective, Open-label, Single Center, Dose Finding Phase I-Study with Atu027 (an siRNA Formulation) in Subjects with Advanced Solid Cancer, https://clinicaltrials.gov/ct2/show/NCT009385742009.
[55] S. Ltd, Phase I—Escalating Dose Study of siG12D LODER (Local Drug EluteR) in Patients With Locally Advanced Adenocarcinoma of the Pancreas, and a Single Dose Study of siG12D LODER (Local Drug EluteR) in Patients With Non-operable Adenocarcinoma of the Pancreas, https://clinicaltrials.gov/ct2/show/NCT011887852010.
[56] N.C.I. (NCI), A Phase 1 Dose Escalation Study of Hepatic Intra-Arterial Administration of TKM 080301 (Lipid Nanoparticles Containing siRNA Against the PLK1 Gene Product) in Patients with Colorectal, Pancreas, Gastric, Breast, Ovarian and Esophageal Cancers with Hepatic, https://clinicaltrials.gov/ct2/show/NCT014370072011.
[57] N.D. Corporation, A Phase 1b/2, Open Label, Randomized, Repeat Dose, Dose Escalation Study to Evaluate the Safety, Tolerability, Biological Activity, and Pharmacokinetics of ND-L02-s0201 Injection, a Vitamin A-coupled Lipid Nanoparticle Containing siRNA Against HSP47, in Subjects with Moderate to Extensive Hepatic Fibrosis (METAVIR F3-4), https://clinicaltrials.gov/ct2/show/NCT022274592014.
[58] I. Dicerna Pharmaceuticals, Phase I, Multicenter, Cohort Dose Escalation Trial to Determine the Safety, Tolerance, and Maximum Tolerated Dose of DCR-MYC, a Lipid Nanoparticle (LNP)-Formulated Small Inhibitory RNA (siRNA) Oligonucleotide Targeting MYC, in Patients with Refractory Locally Advanced or Metastatic Solid Tumor Malignancies, Multiple Myeloma, or Lymphoma, https://clinicaltrials.gov/ct2/show/NCT021105632014.
[59] C. Pharmaceuticals, A Phase I, Dose-Escalating Study of the Safety of Intravenous CALAA-01 in Adults with Solid Tumors Refractory to Standard-of-Care Therapies, https://clinicaltrials.gov/ct2/show/NCT006890652008.
[60] T.P. Corporation, A Phase 1/2 Dose Escalation Study to Determine the Safety, Pharmacokinetics, and Pharmacodynamics of Intravenous TKM-080301 in Patients with Advanced Solid Tumors, https://clinicaltrials.gov/ct2/show/NCT012622352010.
[61] A. Pharmaceuticals, A Multi-Center, Open Label, Phase 1 Dose-Escalation Trial to Evaluate the Safety, Tolerability, Pharmacokinetics and Pharmacodynamics of Intravenous ALN-VSP02 in Patients with Advanced Solid Tumors with Liver Involvement, https://clinicaltrials.gov/ct2/show/NCT008821802009.
[62] A. Pharmaceuticals, A Multi-center, Open-Label, Extension Study of ALN-VSP02 in Cancer Patients Who Have Responded to ALN-VSP02 Treatment, https://clinicaltrials.gov/ct2/show/NCT011580792009.
[63] M. Aleku, P. Schulz, O. Keil, A. Santel, U. Schaeper, B. Dieckhoff, O. Janke, J. Endruschat, B. Durieux, N. Roder, K. Loffler, C. Lange, M. Fechtner, K. Mopert, G. Fisch, S. Dames, W. Arnold, K. Jochims, K. Giese, B. Wiedenmann, A. Scholz, J. Kaufmann, Atu027, a liposomal small interfering RNA formulation targeting protein kinase N3, inhibits cancer progression, Cancer Res. 68 (2008) 9788–9798.
[64] A. Santel, M. Aleku, N. Roder, K. Mopert, B. Durieux, O. Janke, O. Keil, J. Endruschat, S. Dames, C. Lange, M. Eisermann, K. Loffler, M. Fechtner, G. Fisch, C. Vank, U. Schaeper, K. Giese, J. Kaufmann, Atu027 prevents pulmonary metastasis in experimental and spontaneous mouse metastasis models, Clin. Cancer Res. 16 (2010) 5469–5480.
[65] F. Leenders, K. Mopert, A. Schmiedeknecht, A. Santel, F. Czauderna, M. Aleku, S. Penschuck, S. Dames, M. Sternberger, T. Rohl, A. Wellmann, W. Arnold, K. Giese, J. Kaufmann, A. Klippel, PKN3 is required for malignant prostate cell growth downstream of activated PI 3-kinase, EMBO J. 23 (2004) 3303–3313.
[66] D. Strumberg, B. Schultheis, U. Traugott, C. Vank, A. Santel, O. Keil, K. Giese, J. Kaufmann, J. Drevs, Phase I clinical development of Atu027, a siRNA formulation targeting PKN3 in patients with advanced solid tumors, Int. J. Clin. Pharmacol. Ther. 50 (2012) 76–78.
[67] B. Schultheis, D. Strumberg, A. Santel, C. Vank, F. Gebhardt, O. Keil, C. Lange, K. Giese, J. Kaufmann, M. Khan, J. Drevs, First-in-human phase I study of the liposomal RNA Interference therapeutic Atu027 in patients with advanced solid tumors, J. Clin. Oncol. 32 (2014) 4141–4148.
[68] A. Blangy, H.A. Lane, P. d'Herin, M. Harper, M. Kress, E.A. Nigg, Phosphorylation by p34cdc2 regulates spindle association of human Eg5, a kinesin-related motor essential for bipolar spindle formation in vivo, Cell 83 (1995) 1159–1169.
[69] J. Itakura, T. Ishiwata, B. Shen, M. Kornmann, M. Korc, Concomitant overexpression of vascular endothelial growth factor and its receptors in pancreatic cancer, Int. J. Cancer 85 (2000) 27–34.
[70] C.A. Boocock, D.S. Charnockjones, A.M. Sharkey, J. Mclaren, P.J. Barker, K.A. Wright, P.R. Twentyman, S.K. Smith, Expression of vascular endothelial growth-factor and its receptors Flt and Kdr in ovarian-carcinoma, J. Natl. Cancer Inst. 87 (1995) 506–516.
[71] N. Ferrara, H.P. Gerber, J. LeCouter, The biology of VEGF and its receptors, Nat. Med. 9 (2003) 669–676.
[72] M.S. Duxbury, H. Ito, M.J. Zinner, S.W. Ashley, E.E. Whang, RNA interference targeting the M2 subunit of ribonucleotide reductase enhances pancreatic adenocarcinoma chemosensitivity to gemcitabine, Oncogene 23 (2004) 1539–1548.
[73] Y.X. Wang, C.K. Ng, The impact of quantitative imaging in medicine and surgery: charting our course for the future, Quant. Imaging. Med. Surg. 1 (2011) 1–3.
[74] V.K. Tracy Zimmermann, Jamie Harrop, Amy Chan, Joseph Chiesa, Gary Peters, Rick Falzone, Jeffrey Cehelsky, Saraswathy Nochur, Akshay Vaishnaw, Jared Gollob, Phase I First-in-Human Trial of ALN-TTRsc, a Novel RNA Interference Therapeutic for the Treatment of Familial Amyloidotic Cardiomyopathy (FAC), http://www.alnylam.com/web/wp-content/uploads/2013/09/ALN-TTRsc-PhI-HFSA-Poster-Sep2013.pdf2013.
[75] K. Buyens, S.C. De Smedt, K. Braeckmans, J. Demeester, L. Peeters, L.A. van Grunsven, X.D. du Jeu, R. Sawant, V. Torchilin, K. Farkasova, M. Ogris, N.N. Sanders, Liposome based systems for systemic siRNA delivery: stability in blood sets the requirements for optimal carrier design, J. Control. Release 158 (2012) 362–370.
[76] R. Kanasty, J.R. Dorkin, A. Vegas, D. Anderson, Delivery materials for siRNA therapeutics, Nat. Mater. 12 (2013) 967–977.
[77] Y.K. Oh, T.G. Park, siRNA delivery systems for cancer treatment, Adv. Drug Deliv. Rev. 61 (2009) 850–862.
[78] H. Yin, R.L. Kanasty, A.A. Eltoukhy, A.J. Vegas, J.R. Dorkin, D.G. Anderson, Non-viral vectors for gene-based therapy, Nat. Rev. Genet. 15 (2014) 541–555.
[79] P. Zhang, Y. Chen, Y. Zeng, C. Shen, R. Li, Z. Guo, S. Li, Q. Zheng, C. Chu, Z. Wang, Z. Zheng, R. Tian, S. Ge, X. Zhang, N.S. Xia, G. Liu, X. Chen, Virus-mimetic nanovesicles as a versatile antigen-delivery system, Proc. Natl. Acad. Sci. U. S. A. 112 (2015) E6129–E6138.
[80] H. Kobayashi, R. Watanabe, P.L. Choyke, Improving conventional enhanced permeability and retention (EPR) effects; what Is the appropriate Target? Theranostics. 4 (2014) 81–89.
[81] Y. Matsumura, H. Maeda, A new concept for macromolecular therapeutics in cancer-chemotherapy—mechanism of tumoritropic accumulation of proteins and the antitumor agent Smancs, Cancer Res. 46 (1986) 6387–6392.
[82] S.M. Moghimi, A.C. Hunter, J.C. Murray, Long-circulating and target-specific nanoparticles: theory to practice, Pharmacol. Rev. 53 (2001) 283–318.
[83] K.J. Cho, X. Wang, S.M. Nie, Z. Chen, D.M. Shin, Therapeutic nanoparticles for drug delivery in cancer, Clin. Cancer Res. 14 (2008) 1310–1316.
[84] L.E. van Vlerken, T.K. Vyas, M.M. Amiji, Poly(ethylene glycol)-modified nanocarriers for tumor-targeted and intracellular delivery, Pharm. Res. 24 (2007) 1405–1414.
[85] I. Maclachlan, P. Cullis, Diffusible-PEG-lipid stabilized plasmid lipid particles, Adv. Genet. (2005) 157–188 53pa.
[86] P. Vaupel, F. Kallinowski, P. Okunieff, Blood-flow, oxygen and nutrient supply, and metabolic microenvironment of human-tumors—a review, Cancer Res. 49 (1989) 6449–6465.
[87] L. Li, R. Wang, D. Wilcox, X. Zhao, J. Song, X. Lin, W.M. Kohlbrenner, S.W. Fesik, Y. Shen, Tumor vasculature is a key determinant for the efficiency of nanoparticle-mediated siRNA delivery, Gene Ther. 19 (2012) 775–780.
[88] K. Huang, H. Ma, J. Liu, S. Huo, A. Kumar, T. Wei, X. Zhang, S. Jin, Y. Gan, P.C. Wang, S. He, X. Zhang, X.J. Liang, Size-dependent localization and penetration of ultrasmall gold nanoparticles in cancer cells, multicellular spheroids, and tumors in vivo, ACS Nano 6 (2012) 4483–4493.
[89] L. Cunha, K. Szigeti, D. Mathe, L.F. Metello, The role of molecular imaging in modern drug development, Drug Discov. Today 19 (2014) 936–948.
[90] B.R. Meade, S.F. Dowdy, Exogenous siRNA delivery using peptide transduction domains/cell penetrating peptides, Adv. Drug Deliv. Rev. 59 (2007) 134–140.
[91] D.B. Rozema, D.L. Lewis, D.H. Wakefield, S.C. Wong, J.J. Klein, P.L. Roesch, S.L. Bertin, T.W. Reppen, Q. Chu, A.V. Blokhin, J.E. Hagstrom, J.A. Wolff, Dynamic polyconjugates for targeted in vivo delivery of siRNA to hepatocytes, Proc. Natl. Acad. Sci. U. S. A. 104 (2007) 12982–12987.

[92] A.L. Cardoso, S. Simoes, L.P. de Almeida, J. Pelisek, C. Culmsee, E. Wagner, M.C. Pedroso de Lima, siRNA delivery by a transferrin-associated lipid-based vector: a non-viral strategy to mediate gene silencing, J. Gene Med. 9 (2007) 170–183.
[93] T.C. Chu, K.Y. Twu, A.D. Ellington, M. Levy, Aptamer mediated siRNA delivery, Nucleic Acids Res. 34 (2006), e73.
[94] C. Lorenzer, M. Dirin, A.M. Winkler, V. Baumann, J. Winkler, Going beyond the liver: progress and challenges of targeted delivery of siRNA therapeutics, J. Control. Release 203 (2015) 1–15.
[95] J. Gruenberg, F.G. van der Goot, Mechanisms of pathogen entry through the endosomal compartments, Nat. Rev. Mol. Cell Biol. 7 (2006) 495–504.
[96] N.D. Sonawane, F.C. Szoka Jr., A.S. Verkman, Chloride accumulation and swelling in endosomes enhances DNA transfer by polyamine-DNA polyplexes, J. Biol. Chem. 278 (2003) 44826–44831.
[97] O. Boussif, F. Lezoualc'h, M.A. Zanta, M.D. Mergny, D. Scherman, B. Demeneix, J.P. Behr, A versatile vector for gene and oligonucleotide transfer into cells in culture and in vivo: polyethylenimine, Proc. Natl. Acad. Sci. U. S. A. 92 (1995) 7297–7301.
[98] S. Qiu, C.M. Adema, T. Lane, A computational study of off-target effects of RNA interference, Nucleic Acids Res. 33 (2005) 1834–1847.
[99] A. Goodchild, N. Nopper, A. King, T. Doan, M. Tanudji, G.M. Arndt, M. Poidinger, L.P. Rivory, T. Passioura, Sequence determinants of innate immune activation by short interfering RNAs, BMC Immunol. 10 (2009) 40.
[100] A.D. Judge, V. Sood, J.R. Shaw, D. Fang, K. McClintock, I. MacLachlan, Sequence-dependent stimulation of the mammalian innate immune response by synthetic siRNA, Nat. Biotechnol. 23 (2005) 457–462.
[101] M. Sioud, Does the understanding of immune activation by RNA predict the design of safe siRNAs? Front. Biosci. 13 (2008) 4379–4392.
[102] E.M. Sevick-Muraca, J.P. Houston, M. Gurfinkel, Fluorescence-enhanced, near infrared diagnostic imaging with contrast agents, Curr. Opin. Chem. Biol. 6 (2002) 642–650.
[103] J.V. Frangioni, In vivo near-infrared fluorescence imaging, Curr. Opin. Chem. Biol. 7 (2003) 626–634.
[104] P. Zanzonico, Noninvasive imaging for supporting basic research, Small Animal Imaging: Basics and Practical Guide 2011, pp. 3–16.
[105] F. Leblond, S.C. Davis, P.A. Valdés, B.W. Pogue, Pre-clinical whole-body fluorescence imaging: review of instruments, methods and applications, J. Photochem. Photobiol., B 98 (2010) 77–94.
[106] Z. Guo, S. Park, J. Yoon, I. Shin, Recent progress in the development of near-infrared fluorescent probes for bioimaging applications, Chem. Soc. Rev. 43 (2014) 16–29.
[107] S.H. Kim, J.H. Jeong, S.H. Lee, S.W. Kim, T.G. Park, Local and systemic delivery of VEGF siRNA using polyelectrolyte complex micelles for effective treatment of cancer, J. Control. Release 129 (2008) 107–116.
[108] J. Gilleron, W. Querbes, A. Zeigerer, A. Borodovsky, G. Marsico, U. Schubert, K. Manygoats, S. Seifert, C. Andree, M. Stoter, H. Epstein-Barash, L. Zhang, V. Koteliansky, K. Fitzgerald, E. Fava, M. Bickle, Y. Kalaidzidis, A. Akinc, M. Maier, M. Zerial, Image-based analysis of lipid nanoparticle-mediated siRNA delivery, intracellular trafficking and endosomal escape, Nat. Biotechnol. 31 (2013) 638–646.
[109] E. Chang, M.Q. Zhu, R. Drezek, Novel siRNA-based molecular beacons for dual imaging and therapy, Biotechnol. J. 2 (2007) 422–425.
[110] R.J. Christie, Y. Matsumoto, K. Miyata, T. Nomoto, S. Fukushima, K. Osada, J. Halnaut, F. Pittella, H.J. Kim, N. Nishiyama, K. Kataoka, Targeted polymeric micelles for siRNA treatment of experimental cancer by intravenous injection, ACS Nano 6 (2012) 5174–5189.
[111] R.J. Christie, K. Miyata, Y. Matsumoto, T. Nomoto, D. Menasco, T.C. Lai, M. Pennisi, K. Osada, S. Fukushima, N. Nishiyama, Y. Yamasaki, K. Kataoka, Effect of polymer structure on micelles formed between siRNA and cationic block copolymer comprising thiols and amidines, Biomacromolecules 12 (2011) 3174–3185.
[112] Y. Oe, R.J. Christie, M. Naito, S.A. Low, S. Fukushima, K. Toh, Y. Miura, Y. Matsumoto, N. Nishiyama, K. Miyata, K. Kataoka, Actively-targeted polyion complex micelles stabilized by cholesterol and disulfide cross-linking for systemic delivery of siRNA to solid tumors, Biomaterials 35 (2014) 7887–7895.
[113] A.A. Chen, A.M. Derfus, S.R. Khetani, S.N. Bhatia, Quantum dots to monitor RNAi delivery and improve gene silencing, Nucleic Acids Res. 33 (2005), e190.
[114] J. Wang, P. Zhang, C. Huang, G. Liu, K.C. Leung, Y.X. Wang, High performance photoluminescent carbon dots for In Vitro and In vivo bioimaging: effect of nitrogen doping ratios, Langmuir 31 (2015) 8063–8073.
[115] S. Jiang, Y. Zhang, K.M. Lim, E.K.W. Sim, L. Ye, NIR-to-visible upconversion nanoparticles for fluorescent labeling and targeted delivery of siRNA, Nanotechnology 20 (2009), e155101.
[116] J. Jung, A. Solanki, K.A. Memoli, K. Kamei, H. Kim, M.A. Drahl, L.J. Williams, H.R. Tseng, K. Lee, Selective inhibition of human brain tumor cells through multifunctional quantum-dot-based siRNA delivery, Angew. Chem. Int. Ed. 49 (2010) 103–107.
[117] J. Wang, G. Liu, K.C. Leung, R. Loffroy, P.X. Lu, Y.X. Wang, Opportunities and challenges of fluorescent carbon dots in translational optical imaging, Curr. Pharm. Des. 21 (2015) 5401–5416.
[118] L. Wang, X. Wang, A. Bhirde, J. Cao, Y. Zeng, X. Huang, Y. Sun, G. Liu, X. Chen, Carbon-dot-based two-photon visible nanocarriers for safe and highly efficient delivery of siRNA and DNA, Adv. Healthc. Mater. 3 (2014) 1203–1209.
[119] D.K. Chatterjee, Y. Gnanasammandhan, Mk Fau-Zhang, Y. Zhang, Small upconverting fluorescent nanoparticles for biomedical applications, Small 6 (2010) 2781–2795.
[120] L. Wang, J. Liu, Y. Dai, Q. Yang, Y. Zhang, P. Yang, Z. Cheng, H. Lian, C. Li, Z. Hou, P. Ma, J. Lin, Efficient gene delivery and multimodal imaging by lanthanide-based upconversion nanoparticles, Langmuir 30 (2014) 13042–13051.
[121] T.R. Nayak, L.K. Krasteva, W. Cai, Multimodality imaging of RNA Interference, Curr. Med. Chem. 20 (2013) 3664–3675.
[122] A.P. McCaffrey, L. Meuse, T.T. Pham, D.S. Conklin, G.J. Hannon, M.A. Kay, RNA interference in adult mice, Nature 418 (2002) 38–39.
[123] D.L. Lewis, J.E. Hagstrom, A.G. Loomis, J.A. Wolff, H. Herweijer, Efficient delivery of siRNA for inhibition of gene expression in postnatal mice, Nat. Genet. 32 (2002) 107–108.
[124] A. Pichler, N. Zelcer, J.L. Prior, A.J. Kuil, D. Piwnica-Worms, In vivo RNA interference-mediated ablation of MDR1 P-glycoprotein, Clin. Cancer Res. 11 (2005) 4487–4494.
[125] F. Pittella, H. Cabral, Y. Maeda, P. Mi, S. Watanabe, H. Takemoto, H.J. Kim, N. Nishiyama, K. Miyata, K. Kataoka, Systemic siRNA delivery to a spontaneous pancreatic tumor model in transgenic mice by PEGylated calcium phosphate hybrid micelles, J. Control. Release 178 (2014) 18–24.
[126] D.W. Bartlett, M.E. Davis, Insights into the kinetics of siRNA-mediated gene silencing from live-cell and live-animal bioluminescent imaging, Nucleic Acids Res. 34 (2006) 322–333.
[127] S.H. Kim, H. Mok, J.H. Jeong, S.W. Kim, T.G. Park, Comparative evaluation of target-specific GFP gene silencing efficiencies for antisense ODN, synthetic siRNA, and siRNA plasmid complexed with PEI-PEG-FOL conjugate, Bioconjug. Chem. 17 (2006) 241–244.
[128] R. Huschka, A. Barhoumi, Q. Liu, J.A. Roth, L. Ji, N.J. Halas, Gene silencing by gold nanoshell-mediated delivery and laser-triggered release of antisense oligonucleotide and siRNA, ACS Nano 6 (2012) 7681–7691.
[129] M.L. James, S.S. Gambhir, A molecular imaging primer: modalities, imaging agents, and applications, Physiol. Rev. 92 (2012) 897–965.
[130] M.E. Phelps, Positron emission tomography provides molecular imaging of biological processes, Proc. Natl. Acad. Sci. U. S. A. 97 (2000) 9226–9233.
[131] S.I. Ziegler, Positron emission tomography: principles, technology, and recent developments, Nucl. Phys. A. 752 (2005) 679c–687c.
[132] T. Lammers, S. Aime, W.E. Hennink, G. Storm, F. Kiessling, Theranostic nanomedicine, Acc. Chem. Res. 44 (2011) 1029–1038.
[133] W. Lu, G. Zhang, R. Zhang, L.G. Flores 2nd, Q. Huang, J.G. Gelovani, C. Li, Tumor site-specific silencing of NF-kappaB p65 by targeted hollow gold nanosphere-mediated photothermal transfection, Cancer Res. 70 (2010) 3177–3188.
[134] T.R. Nayak, L.K. Krasteva, W. Cai, Multimodality imaging of RNA interference, Curr. Med. Chem. 20 (2013) 3664–3675.
[135] K. Hatanaka, T. Asai, H. Koide, E. Kenjo, T. Tsuzuku, N. Harada, H. Tsukada, N. Oku, Development of double-stranded siRNA labeling method using positron emitter and its in vivo trafficking analyzed by positron emission tomography, Bioconjug. Chem. 21 (2010) 756–763.
[136] F.M. Lu, Z. Yuan, PET/SPECT molecular imaging in clinical neuroscience: recent advances in the investigation of CNS diseases, Quant. Imaging. Med. Surg. 5 (2015) 433–447.
[137] N. Liu, H. Ding, J.L. Vanderheyden, Z. Zhu, Y. Zhang, Radiolabeling small RNA with technetium-99 m for visualizing cellular delivery and mouse biodistribution, Nucl. Med. Biol. 34 (2007) 399–404.
[138] O.M. Merkel, D. Librizzi, A. Pfestroff, T. Schurrat, M. Behe, T. Kissel, In vivo SPECT and real-time gamma camera imaging of biodistribution and pharmacokinetics of siRNA delivery using an optimized radiolabeling and purification procedure, Bioconjug. Chem. 20 (2009) 174–182.
[139] W. Faulkner, Basic Principles of MRIOutSource 1996.
[140] Y.X. Wang, Superparamagnetic iron oxide based MRI contrast agents: current status of clinical application, Quant. Imaging. Med. Surg. 1 (2011) 35–40.
[141] H. Mok, O. Veiseh, C. Fang, F.M. Kievit, F.Y. Wang, J.O. Park, M. Zhang, pH-sensitive siRNA nanovector for targeted gene silencing and cytotoxic effect in cancer cells, Mol. Pharm. 7 (2010) 1930–1939.
[142] M. Shen, F. Gong, P. Pang, K. Zhu, X. Meng, C. Wu, J. Wang, H. Shan, X. Shuai, An MRI-visible non-viral vector for targeted Bcl-2 siRNA delivery to neuroblastoma, Int. J. Nanomedicine 7 (2012) 3319–3332.
[143] C. Li, M.F. Penet, F. Wildes, T. Takagi, Z.H. Chen, P.T. Winnard, D. Artemov, Z.M. Bhujwalla, Nanoplex delivery of siRNA and prodrug enzyme for multimodality image-guided molecular pathway targeted cancer therapy, ACS Nano 4 (2010) 6707–6716.
[144] K.H. Bae, K. Lee, C. Kim, T.G. Park, Surface functionalized hollow manganese oxide nanoparticles for cancer targeted siRNA delivery and magnetic resonance imaging, Biomaterials 32 (2011) 176–184.
[145] Z. Zhou, D. Huang, J. Bao, Q. Chen, G. Liu, Z. Chen, X. Chen, J. Gao, A synergistically enhanced T(1)–T(2) dual-modal contrast agent, Adv. Mater. 24 (2012) 6223–6228.
[146] X. Wang, Z. Zhou, Z. Wang, Y. Xue, Y. Zeng, J. Gao, L. Zhu, X. Zhang, G. Liu, X. Chen, Gadolinium embedded iron oxide nanoclusters as T1–T2 dual-modal MRI-visible vectors for safe and efficient siRNA delivery, Nanoscale. 5 (2013) 8098–8104.
[147] H.D. Liang, M.J.K. Blomley, The role of ultrasound in molecular imaging, Br. J. Radiol. 76 (2003) S140–S150.
[148] M.S. Shim, Y.J. Kwon, Stimuli-responsive polymers and nanomaterials for gene delivery and imaging applications, Adv. Drug Deliv. Rev. 64 (2012) 1046–1059.
[149] E. Unger, T. Porter, J. Lindner, P. Grayburn, Cardiovascular drug delivery with ultrasound and microbubbles, Adv. Drug Deliv. Rev. 72 (2014) 110–126.
[150] K.H. Martin, P.A. Dayton, Current status and prospects for microbubbles in ultrasound theranostics, Wiley Interdiscip. Rev. Nanomed. Nanobiotechnol. 5 (2013) 329–345.
[151] S. Florinas, J. Kim, K. Nam, M.M. Janat-Amsbury, S.W. Kim, Ultrasound-assisted siRNA delivery via arginine-grafted bioreducible polymer and microbubbles targeting VEGF for ovarian cancer treatment, J. Control. Release 183 (2014) 1–8.
[152] R.E. Vandenbroucke, I. Lentacker, J. Demeester, S.C. De Smedt, N.N. Sanders, Ultrasound assisted siRNA delivery using PEG-siPlex loaded microbubbles, J. Control. Release 126 (2008) 265–273.

[153] Y. Liu, H. Miyoshi, M. Nakamura, Encapsulated ultrasound microbubbles: therapeutic application in drug/gene delivery, J. Control. Release 114 (2006) 89–99.
[154] C.C. Chen, P.S. Sheeran, S.Y. Wu, O.O. Olumolade, P.A. Dayton, E.E. Konofagou, Targeted drug delivery with focused ultrasound-induced blood–brain barrier opening using acoustically-activated nanodroplets, J. Control. Release 172 (2013) 795–804.
[155] X. Cheng, H. Li, Y. Chen, B. Luo, X. Liu, W. Liu, H. Xu, X. Yang, Ultrasound-triggered phase transition sensitive magnetic fluorescent nanodroplets as a multimodal imaging contrast agent in rat and mouse model, PLoS ONE 8 (2013), e85003.
[156] P.A. Dayton, S. Zhao, S.H. Bloch, P. Schumann, K. Penrose, T.O. Matsunaga, R. Zutshi, A. Doinikov, K.W. Ferrara, Application of ultrasound to selectively localize nanodroplets for targeted imaging and therapy, Mol. Imaging 5 (2006) 160–174.
[157] J. Jian, C. Liu, Y. Gong, L. Su, B. Zhang, Z. Wang, D. Wang, Y. Zhou, F. Xu, P. Li, Y. Zheng, L. Song, X. Zhou, India ink incorporated multifunctional phase-transition nanodroplets for photoacoustic/ultrasound dual-modality imaging and photoacoustic effect based tumor therapy, Theranostics. 4 (2014) 1026–1038.
[158] S. Horie, Y. Watanabe, M. Ono, S. Mori, T. Kodama, Evaluation of antitumor effects following tumor necrosis factor-alpha gene delivery using nanobubbles and ultrasound, Cancer Sci. 102 (2011) 2082–2089.
[159] C.H. Wang, Y.F. Huang, C.K. Yeh, Aptamer-conjugated nanobubbles for targeted ultrasound molecular imaging, Langmuir 27 (2011) 6971–6976.
[160] T. Yin, P. Wang, J. Li, Y. Wang, B. Zheng, R. Zheng, D. Cheng, X. Shuai, Tumor-penetrating codelivery of siRNA and paclitaxel with ultrasound-responsive nanobubbles hetero-assembled from polymeric micelles and liposomes, Biomaterials 35 (2014) 5932–5943.
[161] Z. Chen, K. Liang, J. Liu, M. Xie, X. Wang, Q. Lu, J. Zhang, L. Fang, Enhancement of survivin gene downregulation and cell apoptosis by a novel combination: liposome microbubbles and ultrasound exposure, Med. Oncol. 26 (2009) 491–500.
[162] J. Castle, M. Butts, A. Healey, K. Kent, M. Marino, S.B. Feinstein, Ultrasound-mediated targeted drug delivery: recent success and remaining challenges, Am. J. Physiol. Heart Circ. Physiol. 304 (2013) H350–H357.
[163] O.F. Kaneko, J.K. Willmann, Ultrasound for molecular imaging and therapy in cancer, Quant. Imaging. Med. Surg. 2 (2012) 87–97.
[164] S. Son, H.S. Min, D.G. You, B.S. Kim, I.C. Kwon, Echogenic nanoparticles for ultrasound technologies: evolution from diagnostic imaging modality to multimodal theranostic agent, Nano Today 9 (2014) 525–540.
[165] V. Sboros, Response of contrast agents to ultrasound, Adv. Drug Deliv. Rev. 60 (2008) 1117–1136.
[166] A.R. Carson, C.F. McTiernan, L. Lavery, M. Grata, X. Leng, J. Wang, X. Chen, F.S. Villanueva, Ultrasound-targeted microbubble destruction to deliver siRNA cancer therapy, Cancer Res. 72 (2012) 6191–6199.
[167] Q.-L. Zhou, Z.-Y. Chen, Y.-X. Wang, F. Yang, Y. Lin, Y.-Y. Liao, Ultrasound-mediated local drug and gene delivery using nanocarriers, Biomed. Res. Int. (2014), e963891.
[168] T. Yin, P. Wang, J. Li, R. Zheng, B. Zheng, D. Cheng, R. Li, J. Lai, X. Shuai, Ultrasound-sensitive siRNA-loaded nanobubbles formed by hetero-assembly of polymeric micelles and liposomes and their therapeutic effect in gliomas, Biomaterials 34 (2013) 4532–4543.
[169] D.E. Lee, H. Koo, I.C. Sun, J.H. Ryu, K. Kim, I.C. Kwon, Multifunctional nanoparticles for multimodal imaging and theragnosis, Chem. Soc. Rev. 41 (2012) 2656–2672.
[170] H.S. Choi, J.V. Frangioni, Nanoparticles for biomedical imaging: fundamentals of clinical translation, Mol. Imaging 9 (2010) 291–310.
[171] A.Y. Louie, Multimodality imaging probes: design and challenges, Chem. Rev. 110 (2010) 3146–3195.
[172] O.C. Boerman, W.J.G. Oyen, Multimodality probes: amphibian cars for molecular imaging, J. Nucl. Med. 49 (2008) 1213–1214.
[173] J.M. Idee, S. Louguet, S. Ballet, C. Corot, Theranostics and contrast-agents for medical imaging: a pharmaceutical company viewpoint, Quant. Imaging. Med. Surg. 3 (2013) 292–297.
[174] Y.X. Wang, Physical scientists research biomedicine: a call for caution, Chin. J. Cancer Res. 27 (2015) 94–95.
[175] Z. Medarova, W. Pham, C. Farrar, V. Petkova, A. Moore, In vivo imaging of siRNA delivery and silencing in tumors, Nat. Med. 13 (2007) 372–377.
[176] M. Mikhaylova, I. Stasinopoulos, Y. Kato, D. Artemov, Z.M. Bhujwalla, Imaging of cationic multifunctional liposome-mediated delivery of COX-2 siRNA, Cancer Gene Ther. 16 (2009) 217–226.
[177] D.W. Bartlett, H. Su, I.J. Hildebrandt, W.A. Weber, M.E. Davis, Impact of tumor-specific targeting on the biodistribution and efficacy of siRNA nanoparticles measured by multimodality in vivo imaging, Proc. Natl. Acad. Sci. U. S. A. 104 (2007) 15549–15554.
[178] Y.X.J. Wang, Y. Choi, Z.Y. Chen, S. Laurent, S.L. Gibbs, Molecular imaging: from bench to clinic, Biomed. Res. Int. 2014 (2014) 357258.